SAHLGRENSKA ACADEMY

ESTIMATION OF RADIATION EXPOSURE FROM NATURALLY OCCURRING RADIONUCLIDES IN FOOD AND FOODSTUFF

Ida Bengtson

Essay/Thesis:	30 hp
Program and/or course:	Medical Physics
Level:	Second Cycle
Semester/year:	Autumn 2018
Supervisor:	Francisco Piñero García and Mats Isaksson
Examiner:	Magnus Båth

Abstract

Essay/Thesis:	30 hp
Program and/or course:	Medical Physics
Level:	Second Cycle
Semester/year:	Autumn 2018
Supervisor:	Francisco Piñero García and Mats Isaksson
Examiner:	Magnus Båth
Keyword:	Naturally occurring radionuclides, committed effective dose from ingested radionuclides, biokinetic models

---

Purpose: The main purpose of this study was to provide an estimation of the committed effective dose received by the Swedish population from naturally occurring radionuclides (NORM) in the diet. This study was also aiming to investigate the impact on the committed effective dose due to the new developments in the biokinetic model for ^{210}Po. In addition to dose estimation, this project was also aiming to investigate how to make interpolation maps using the software ArcGIS.

Background & theory: In previous studies of radioactivity in food, the focus has been on anthropogenic radionuclides. Even though NORM in food is contributing to a larger committed effective dose than anthropogenic radionuclides, no detailed assessment of the committed effective dose from NORM to the Swedish population has been done. For ^{210}Po, which is an important radionuclide for the committed effective dose from the diet, new developments have been done in the systemic model. One of the new developments include an additional excretion pathway, via hair and sweat.

Method: Activity concentrations of ^{210}Po, ^{234}U and ^{238}U in various food and foodstuff were collected from the ongoing research projects *Radiological Implications of Swedish Food Consumption* and *Natural radioactivity in the Nordic diet*. Committed effective doses were calculated for adults and children of three age groups. Comparisons were made of committed effective doses received by Swedish men vs. women and also lacto-ovo vegetarians vs. people including animal protein in their diet.

The investigation of the impact on the committed effective dose from ^{210}Po due to new developments in the biokinetics was done using the softwares IMBA, SAAM II and Ecolego. In IMBA, the impact on the committed effective dose was simulated by varying the GI uptake fraction, the tissue weighting factors and the transfer rate between stomach and small intestine. In SAAM II and Ecolego, the biokinetics of ^{210}Po was simulated using the Human Alimentary Tract Model and the updated systemic model. By using the methodology in ICRP 133, the committed effective dose coefficient was calculated and compared with the coefficient from ICRP 119.

The interpolation of dose rate data was carried out in the software ArcGIS 10.6, using the Empirical Bayesian Kriging method.

Results & conclusion:

The committed effective doses received by adults and children were 77 ± 2 μSv/y and 94 ± 9 μSv/y, respectively. The Swedish men receive a 20% higher committed effective dose than the Swedish women. Diet including animal protein results in a 4.5 higher committed effective dose from ^{210}Po than lacto-ovo vegetarian diet. The overall effect of cooking of food is a reduction of the levels of ^{210}Po.

By varying the GI uptake fraction, the estimate of the committed effective dose from ^{210}Po differed by $\pm$ 9% from the dose calculated using the GI uptake fraction defined by ICRP. When using the tissue weighting factors from ICRP 133, the estimate of the committed effective dose from ^{210}Po was 23% higher than the dose calculated using the weighting factors from ICRP 68. When using the sex dependent transfer rates, a higher committed equivalent dose to stomach was estimated for women than men.

The simulation of biokinetics of ^{210}Po suggested that the new developments in the biokinetic models is leading to a 5-18% higher estimation of the committed effective dose from NORM in food received by Swedish adults.

Measured values were compared with predicted values in the interpolated dose rate map. Good agreement was found, suggesting that the Empirical Bayesian Kriging method works well for this purpose.

Table of content

Introduction

Natural radionuclides are occurring in all types of food and foodstuff. The radiation source that food constitutes is rarely concerned as a health risk due to the very low levels of radionuclides [1]. Large variation in the levels of radionuclides are though present in different geographic locations, depending on geology, agriculture procedures and climate. In previous studies, the focus has been on anthropogenic radionuclides in food and not so much on naturally occurring radionuclides (NORM), despite the fact that NORM in food contribute to a higher committed effective dose than the man-made radionuclides.

The annual effective dose received from all natural sources is on average 2.4 mSv for the world population [2]. This includes exposure from radionuclides in bedrock and soil, in food, water and air, cosmic radiation and radionuclides in our bodies. Considering the artificial exposure (dominantly of medical origin) as well, the total committed effective dose to the world population is on average 3 mSv per year. Food consumption is contributing to 0.29 mSv of the yearly dose from natural exposure [3]. The reference level for ingestion doses are set to 1 mSv [1].

The Swedish population is receiving a total annual effective dose of 3.7 mSv to the whole population and 2.4 mSv to never-smokers (2007) [4]. The contribution from NORM in food and foodstuff is 0.2 mSv. For reindeer keepers, the total annual effective dose is 3 mSv. This is due to the additional contribution from NORM in food of 0.8 mSv and the contribution from the Chernobyl fallout of ^{137}Cs in food. The annual effective dose received from ^{137}Cs is 0.18 mSv for reindeer keepers and 0.025 mSv for the whole population.

The International Atomic Energy Agency (IAEA) is working on producing a guide for NORM in food, to complement the existing guides for anthropogenic radioactivity occurring in food [1]. This guide will consist of activity concentrations in various food and foodstuff, information about when higher levels might appear and information about food that contain high activity concentration.

Background

Previous research

In 2017, a study of the annual committed effective dose received by the Norwegian people was carried out. Food was contributing to 10% of the total annual committed effective dose, where 98% was due to radionuclides of natural origin [5]. The radionuclides that were considered to contribute to the committed effective dose were the naturally occurring ^{210}Po, ^{228}Ra, ^{222}Rn, ^{40}K, ^{210}Pb, ^{14}C, ^{226}Ra and the anthropogenic ^{137}Cs. The highest committed effective doses came from ^{210}Po and ^{40}K.

Other NORM that have been found to be important for the committed effective dose are ^{238}U, ^{234}U, ^{230}Th, ^{232}Th, ^{228}Th and ^{224}Ra [6].

Different habits in food consumption can result in higher exposures of certain groups of the population. In the study of the Norwegian diet, the groups examined were the whole population and the special groups that eat high amounts of reindeer meat, sheep meat, wild products (game meat, mushrooms, berries) and seafood [5]. The exposure scenario that contributed the most to the committed effective dose was high consumption of ^{137}Cs contaminated reindeer meat. ^{210}Po in reindeer meat and in seafood was also found to play an important role for the committed effective dose.

The annual effective dose received from the uranium and thorium series in food is 0.12 mSv to adults in the world population, where ^{210}Po is the radionuclide contributing the most [7]. Table 1 shows the annual effective dose to the world population received from radionuclides in the uranium and thorium series in food.

Table 1: Annual effective dose to the world population from radionuclides in the uranium and thorium series in food [7].

Radionuclide	Committed effective dose [$\mu Sv/y$]		
	Infants (1 year)	Children (10 years)	Adults
^{238}U	0.23	0.26	0.25
^{234}U	0.25	0.28	0.28
^{230}Th	0.42	0.48	0.64
^{226}Ra	7.5	12	6.3
^{210}Pb	40	40	21
^{210}Po	180	100	70
^{232}Th	0.26	0.32	0.38
^{228}Ra	31	40	11
^{228}Th	0.38	0.30	0.22
^{235}U	0.011	0.012	0.012

The annual effective dose to the world population from NORM in food is on average 0.29 mSv, where 0.12 mSv is received from the uranium and thorium series and 0.17 mSv is received from ^{40}K [3].

Present research

Radiological Implications of Swedish Food Consumption is an ongoing research project performed at the University of Gothenburg, funded by the Swedish Radiation Safety Authority (SSM). The purpose of the project is to estimate the levels of anthropogenic and natural radionuclides in the Swedish diet. In the project, a database of radioactivity levels in foodstuff will be performed and the radiological risk due to consumption will be estimated. Mixed diets, such as in kindergartens, schools and hospitals will be studied and critical groups will be identified. A study of the origin of foodstuff will also take place, as well as a comparison between radionuclide levels of natural and anthropogenic type. The project aims to determine the fraction of the annual effective dose contributed by food consumption.

The samples of foodstuff will be collected at different locations in Sweden and imported food will be considered as well. The samples include milk products, cereals, vegetables, fruits, meat, fish and other foodstuff. Studies will be performed to examine seasonal differences. Wild food will also be included such as game, mushrooms and berries.

Natural radioactivity in the Nordic diet (NANOD) is a present research project performed as a collaboration between the Nordic countries, supported by Nordic Nuclear Safety Research (NKS). The aim of this project is to extend the knowledge of the levels of NORM in seafood and the committed effective dose received by the Nordic population due to seafood ingestion. The project is of importance because of the high levels of NORM in seafood in combination with the high consumption of fish and shellfish in the Nordic countries. In the project, the effects of storage, preparation and geographic location of the food on the levels of radionuclides will be investigated. The foundation of this project was the study made by Norwegian Scientific Committee for Food Safety in 2017, where they concluded that 98% of the annual committed effective dose from food was due to natural radioactivity [5]. The hypothesis is that this is true for all Nordic countries.

Naturally occurring radionuclides in the environment and in food

^{210}Po is one of the final daughters in the chain of the naturally occurring radionuclide ^{238}U, decaying with a half-life of 138 d [8]. ^{238}U occurs in soil and minerals, resulting in the presence of ^{210}Po deep in the ground [9]. ^{210}Po is also distributed in the atmosphere due to the grandparent ^{222}Rn that exist in gas form. From the atmosphere, ^{210}Po is deposited on the surfaces and vegetation. The amount of deposition varies due to factors such as rain and geographical position. High levels of ^{210}Po are accumulated in marine biota, due to its high

complex formation with proteins and uptake in other internal tissues. ^{210}Po is highly radiotoxic because of its high energy alpha particle emission and high specific activity.

One important pathway for ^{210}Po to enter the human body is via ingestion of reindeer that has eaten lichen containing the radionuclide [10]. Measurements of ^{210}Po in lichen have been carried out in central Sweden since the 1960s. The amount of ^{210}Po fallout has been constant since the measurements started. In the future, the deposition may change though due to climate changes.

Diets including a lot of reindeer and caribou has been found to contain large amounts of ^{210}Po [10]. A strong dependence of seasons is seen in activity concentration in reindeer meat from Lapland, Sweden. In samples from 1969, the activity concentration varied between 3 and 12 Bq/kg with the highest level in spring. People eating high amounts of reindeer or caribou meat is assumed to receive a committed effective dose from ^{210}Po of 260 μSv/y.

In wild leafy vegetation, the highest contribution to the naturally occurring radioactivity is ^{210}Po [10]. In the 1960s, it was found that 80% of the natural radioactivity in plants was ^{210}Po originating from deposition of the nuclide and other ^{222}Rn daughters from air, but also from absorption of ^{210}Po via the roots. One example of a leafy plant consumed by humans is tobacco, in which high levels of ^{210}Po have been found. In the lungs of smokers, the amount of ^{210}Po is three times higher than in non-smokers [7].

Ingestion of ^{210}Po in food is an important contribution to the effective dose to the human being. The intake of ^{210}Po from terrestrial food varies between 10 and 100 Bq/y depending on differences in geology, climate and agriculture [10]. The largest contribution, 80%, of the ingested ^{210}Po is due to fish and shellfish. For example, in Japan and Korea where the diet includes high amounts of seafood, the committed effective dose from ^{210}Po is estimated to 270 μSv/y.

The average of the committed effective dose from ^{210}Po to the world population is assumed to be 70 μSv/y [10]. For vegetarians, the committed effective dose has been estimated to 30 μSv/y. For people who eat high amounts of fish, the committed effective dose can be 5-15 times higher than for vegetarians.

Other NORM, being important for the effective doses received via ingestion, are ^{40}K, ^{238}U and ^{234}U. The physical half-life of ^{40}K is $1.28 \cdot 10^9$ y and some foods are containing high amounts of the nuclide, for example bananas (130 Bq/kg), peanuts (215 Bq/kg) and raw spinach (240 Bq/kg) [11]. K is an important element in the human body and the activity concentration of ^{40}K is 61 Bq/kg body mass [12]. The uptake of potassium is regulated to hold a constant level in the body, therefore any extra intake is excreted [5]. ^{40}K contributes to a constant fraction of all potassium and therefore, the committed effective dose received from ^{40}K is not affected by the amount of intake of potassium.

Uranium occurs in all rocks and soils and in natural watercourse [12]. ^{238}U and ^{234}U have physical half-lives of $4.47 \cdot 10^9$ y and $2.46 \cdot 10^5$ y, respectively. Uranium is often more important as a chemotoxic health risk rather than a radiotoxic. The activity concentration of

uranium is on average 12-37 Bq/kg in the earth's crust and 1.2-12 mBq/kg in water. The occurrence of uranium in food is largely variating but some of the highest concentrations, about 2-3 Bq/kg, of ^{238}U have been found in root vegetables and leafy vegetables [7].

Interpolation maps

The measurement of dose rate or activity concentration in the environment by using a detector in a backpack or in a car, result in data at discrete locations. Making an interpolated map out of this discrete data gives the advantage of a better overview provided over the measured area. This could be useful to quickly find hot spots as well as sorting out safe areas. This in turn, enables the measurement to be focused on the hot spots. In this way the performance gets more efficient and time saving.[1]

Interpolation of dose rate data can also be used to get estimated values at sites where it is hard to measure, for example in tough terrains. Additionally, interpolation is good when the data are to be presented for authorities and the public since it is easier to understand a continuous surface than discrete values.[2]

[1] Mantero Cabrera, Juan; postdoctoral researcher at the department of Radiation Physics at Institute of Clinical Sciences, Sahlgrenska Academy, Gothenburg University, 2018, dialogue in November.
[2] Thomas, Rimon; doctoral student at the department of Radiation Physics at Institute of Clinical Sciences, Sahlgrenska Academy, Gothenburg University, 2018, dialogue in November.

Aim

The aim of this study was to

- estimate the committed effective doses received by the Swedish population due to naturally occurring radionuclides in the Swedish diet
- simulate the biokinetics of polonium and investigate the impact of the new developments in the biokinetic models on the committed effective dose
- produce a manual for interpolation of discrete dose rate data in order to create continuous dose rate maps.

Theory

Internal dosimetry

The assessment of doses due to intake of radionuclides into the body is comprised of measurements of activities followed by modelling, in order to convert the activity to dose. The International Commission on Radiological Protection (ICRP) is providing models required for the assessment [13]. Measurement can be done of the activity of the intake, in the body or in the excreta. The models then describe the distribution of the radionuclides in the body and the energy deposition in the organs. The challenge with internal dosimetry is that the body after the intake is exposed to irradiation where the source is varying in geometry and strength. This is a result of the heterogeneous distribution in the body due to the biokinetic behaviour of the radionuclide, as well as the decrease of activity due to excretion and nuclear decay. The dose quantity in internal dosimetry, committed dose, is taking into account that the exposure is not momentary by integrating the dose over a period of time.

Modelling of the biokinetics of a radionuclide entails the uncertainties originating from biological differences between individuals [13]. There is incomplete knowledge about the processes being modelled and limited ability for calculation of their parameter values. The parameters in the ICRP reference models are set as fixed values and are not associated with any uncertainties. These parameter values have been extracted from human and animal studies.

Measurements of the activity concentration result in sources of uncertainties like estimation of the sample weight, positioning of the source during measurement and contaminations in the sample [13].

Biokinetic models

The distribution and retention of a radionuclide in the body depend on factors such as type of element, its chemical form and route of intake and is described by biokinetic models [13]. The biokinetic models published by ICRP are describing the human body as a compartmental system, thus dividing the body in several compartments, containing activity. Between the compartments activity can pass back and forth. Each compartment can represent an organ, a tissue or a compound of organs. The amount of activity in a compartment is described with first order differential equations.

Metabolic models

To estimate the uptake of radionuclides entering the body via ingestion, the gastrointestinal system has to be modelled. ICRP published a gastrointestinal tract model in 1973 (Figure 1), described in ICRP 30 [14]. The system is described as a compartment model including stomach, small intestine and upper- and lower large intestine. This model was replaced in 2006 by a new compartment model, Human Allimentary Tract Model (HATM) (Figure 2), described in ICRP 100 [15]. The development of the new model took place when better understanding of the transfer of materials in the intestines was obtained, as well as better

knowledge about the sites where the sensitive cells are located [15]. In HATM, the mouth and oesophagus are included as compartments to take into account the possibility of receiving radiation doses in these areas as well. In the ICRP 30 model, the uptake of radionuclides to the blood was considered to take place from the small intestine. In HATM, absorption of radionuclides can occur additionally from the oral cavity, stomach and segments of the colon. The transit time, i.e. the time the radionuclide remains in one compartment, is in the old model independent of age, gender and the type of material that has been ingested. In the new model these things have been considered. The path in HATM starts with entrance of the radionuclide into the oral cavity and further on to the oesophagus, stomach, small intestine, colon and at last excretion via faeces. Radionuclides can also reach the oesophagus through clearance from the respiratory tract. Retention on teeth and in oral mucosa is considered. HATM is a recycling model, allowing the radionuclide to go forth and back for example between the walls in the stomach and the blood.

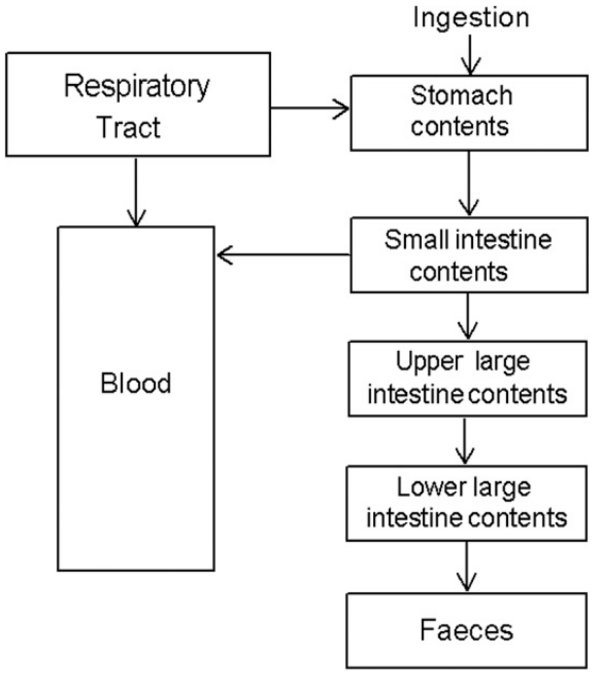

Figure 1: The old gastrointestinal model described in ICRP 30 [15].

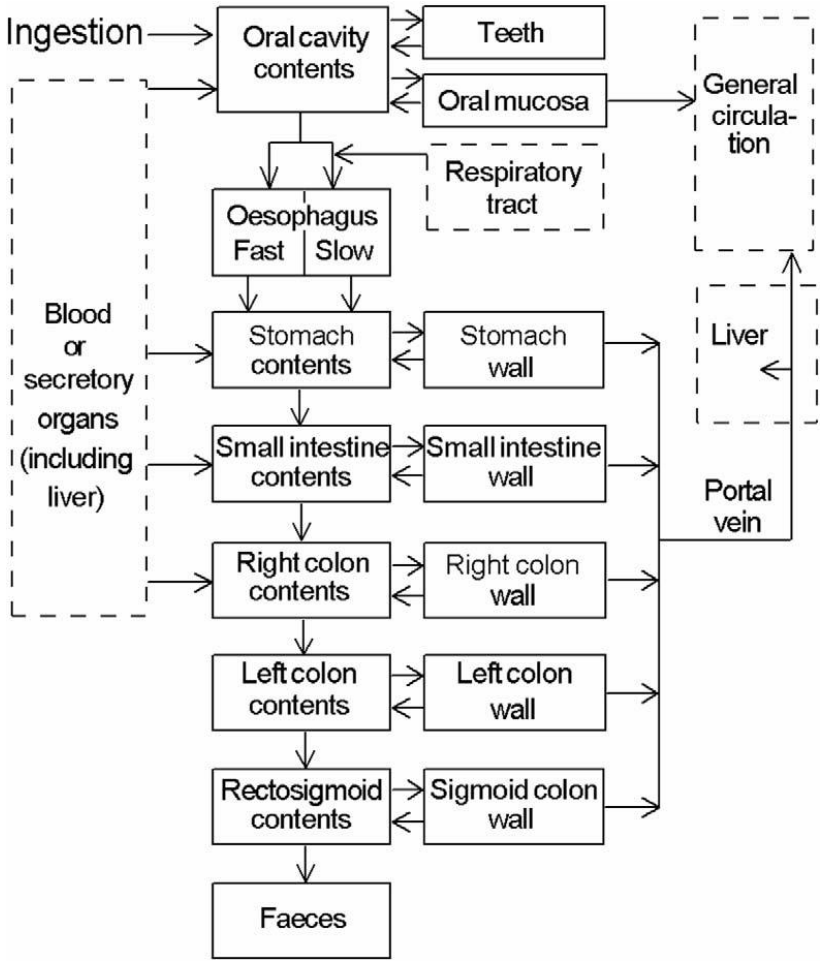

Figure 2: The Human Alimentary Tract Model (HATM) described in ICRP 100 [15].

When a radionuclide is ingested, an amount of the substance will be absorbed to the blood while the rest will maintain in the gastrointestinal tract and later on be excreted. The amount absorbed to the blood is in the old GI model referred to as the GI uptake fraction f_1 and equals the absorbed fraction from the small intestine [15]. In HATM f_1 is replaced by the total absorbed fraction f_A including absorption via other sites in the gastrointestinal tract as well as the small intestine. The standard assumption though is that all absorption is taking place in the small intestine. Since HATM was developed, ICRP has produced committed effective dose coefficients for various elements based on this model, applicable for workers (Publication of occupational intakes of radionuclides (OIR)) [16-18]. For the purpose of dose estimation for the public, dose coefficients based on HATM are yet not elaborated. The current committed effective dose coefficients applicable for the public are based on the old GI model and are presented in the ICRP publication 119 [19]. The committed effective dose coefficients, expressed in Sv/Bq, are calculated using a specific value of f_1 for each element. The GI uptake fraction can be affected by the chemical form of the radionuclide ingested. This can be taken into consideration by modifying the dose coefficients by scaling [5]. The dose coefficients give

the committed effective dose, i.e. the integrated effective dose over a period of time after the intake, 50 years for adults and 70 years for children [19]. This can result in a significant overestimation of the annual dose [5]. For those radionuclides that have a long retention time and thereby deposit energy during several years, the annual dose gets overestimated. For those radionuclides that do not maintain in the body more than a year, the committed effective dose is corresponding to the annual dose.

Systemic models

A systemic model describes the distribution of a radionuclide after it has reached the blood circulation. The new occupational committed effective dose coefficients presented in the publications of OIR [16-18] are based on updates of the systemic models [13]. The development of the systemic models includes the possibility of a recycling radionuclide transport between compartments, unlike in most of the old models, where transport in one direction was the only alternative. Another development in the new systemic models is the modelling of daughter nuclides. Instead of following their mothers' biokinetics as in the old models, they are now modelled independently. An update of the committed effective dose coefficients for the member of public is planned by ICRP, to include improvements done in the Publications of OIR.

Some of the organs and tissues in the systemic models are divided in several compartments to consider the different transit times and retentions that can occur in the same organ or tissue [18]. The function of more than one compartment is also to model the different pathways the radionuclide can take when leaving an organ or a tissue.

Polonium

The systemic model for polonium that was described in ICRP 67 (1993) is assuming that the absorbed radioactivity is distributed and accumulated in the liver (30%), kidneys (10%), spleen (5%), red bone marrow (10%) and the rest of the body (45%) [20]. The biological half-life is 50 days. More than 50% of the polonium that reaches the blood, is excreted via faeces. In 2001, Leggett and Eckerman (L&E) [21] established a new, more realistic biokinetic model, the L&E model (Figure 3). Unlike the model in ICRP 67, the L&E model includes excretion via sweat and hair. The L&E model also includes a compartment for the bone surface as well as a more proper modelling of the excretion in urine [22]. In the Publications of OIR, the L&E model is implemented [18].

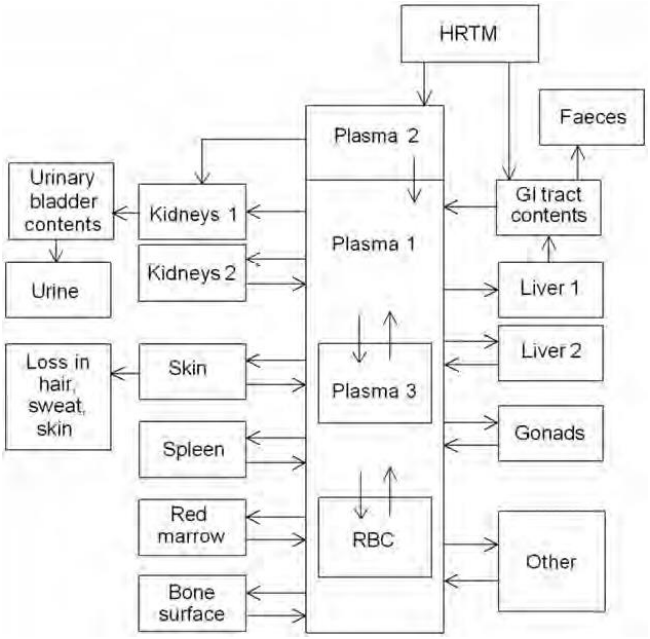

Figure 3: The systemic model for polonium (L&E model) [5]. HRTM: Human Respiratory Tract Model, RBC: Red Blood Cells. The Plasma is modelled as three compartments, Plasma 1, 2 and 3.

When polonium has reached the blood, first a fast decrease in amount is taking place followed by a slower reduction [18]. The liver is receiving a large amount, 35% of the systemic polonium, while 10% is deposited in the kidneys and 2% in the spleen. The skin is receiving 5% of the polonium and half of it is excreted via hair and sweat, while the other half is returned to the blood. The red marrow is receiving 4% and the bone surface 1.5%. The bone surface has the longest retention half-life of the tissues in the body. Other tissues are absorbing 32.4%.

The GI uptake fraction has been studied in several research projects and different values have been estimated: 0.56 ± 0.04 (2001), 0.51 (2007) and 0.46 ± 0.08 (2012) [23]. The biological half-life has also been estimated in different studies: 38 ± 1 d (2001), 42 ± 1 d (2007) and 31 ± 5.5 d (2012) [23].

Uncertainties and limitations in biokinetic models

Uncertainties associated with a biokinetic model can be caused by a model structure that is simplifying the processes too much [24]. Parts in a process that are unknown and thereby not included in the model result in uncertainties. The extent of uncertainties involved in a biokinetic model is variating for different radionuclides, because of the differences in biokinetic knowledge.

In HATM, uncertainties are associated with the radionuclide absorption, the transit times and the anatomical construction [15].

The biokinetics in the human body depends on, for example, the diet and the age of the person. The biokinetics also variates between different humans. There are two types of

variability, defined in ICRP 100, inter-individual variability and intra-individual variability [15]. Inter-individual variability is the differences between persons under similar conditions and intra-individual variability is the differences in one person under different conditions.

Integrated Modules for Bioassay Analysis (IMBA)

Integrated Modules for Bioassay Analysis (IMBA) is a set of software components for estimation of internal doses by using the ICRP biokinetic models [25]. Each software component has a specific function, for example calculating organ doses or approximating the intake of a radionuclide. One component is representing the biokinetic models. The retention $R_s(t)$ in all source organs is described with the same equation, irrespectively of the radionuclide:

$$R_s(t) = \sum_{i=1}^{n} a_i e^{-\lambda_i t} \quad (1)$$

where a_i is a dimensionless amplitude, λ_i $[d^{-1}]$ is the transfer rate, n is the number of exponential terms and t [d] is the time after the entrance of the radionuclide into the organ. At $t = 0$, $R_s(t) = 0$ for all organs and tissues besides the blood that has the retention $R_s(t) = 1$.

Models implemented in IMBA

The models implemented in IMBA are the old gastrointestinal model from ICRP 30 (1979), the non-recycling systemic models from ICRP 30 (1979) and the recycling systemic models from ICRP 56 (1989) [25]. The radiation and tissue weighting factors used in IMBA are those published in ICRP 60 (1991) and ICRP 68 (1994), respectively.

Simulation, Analysis and Modelling Software II (SAAM II)

Simulation, Analysis and Modelling Software II (SAAM II) is a software for compartmental modelling [26]. SAAM II produces a system of first order differential equations from the user defined compartmental model including specific parameters and input values. The output of the model is determined by the software and can be presented to the user in a graphical form.

Ecolego

Ecolego is a software for simulation of models, specialized on estimation of radiological risk [27]. Advantages with Ecolego compared with SAAM II is the built-in function for considering of the physical decay, as well as the greater possibilities of solving the differential equations of the model. Ecolego can solve stiff problems, i.e. models with largely varying

transfer coefficients. Ecolego also has a build-in function for integration of the amount in the simulated model.

The Kriging interpolation method

Kriging is a geostatistical method, which means interpolation considering the statistical relationship between the data points [28]. This results in an interpolation with an estimated uncertainty. Kriging is a good method to use for interpolation of data points that are correlated spatially and is used for example in soil science and geology. The Kriging formula is described as

$$\hat{Z}(s_0) = \sum_{i=1}^{N} \varphi_i Z(s_i), \quad (2)$$

where $\hat{Z}(s_0)$ is the prediction at location s_0, φ_i is a weighting factor for measured value i, $Z(s_i)$ is the measured value at location s_i and N is the number of measured values. The weighting factor φ_i depends on a model fitted to the measured points, the distance to the location of the prediction and the spatial relationship between the measured points.

The first step in Kriging is to investigate the spatial relationship between the data points, by making a semivariogram [28]. For all points i and j separated with distance h, the semivariance S(h) is calculated as

$$S(h) = \frac{1}{2} \cdot average\left((v_i - v_j)^2\right), \quad (3)$$

where v_i and v_j are the values at locations i and j, respectively. The semivariogram is created by plotting the semivariance S as a function of the distance h. The semivariogram is then fitted to a model, where a spherical model is the most used.

The second step is to calculate the weights φ_i using the information from the fitted semivariogram [28]. The values nearest the position of the prediction has the highest influence and the prediction is then made using the Kriging formula.

In ArcGIS 10.6, there are two types of geostatistical methods using the Kriging formula, named Kriging/CoKriging and Empirical Bayesian Kriging (EBK) [28]. There are two main differences between the two methods. In EBK, the Kriging parameters are calculated automatically while in Kriging/CoKriging, you have to select them yourself. EBK gives a better estimate of the errors of the prediction compared with Kriging/CoKriging. This is because the errors in the semivariogram is accounted for in EBK and not in Kriging/CoKriging. The disadvantage with EBK is that the calculation takes longer time than in Kriging/CoKriging.

The Kriging method has been used when making interpolation of the levels of ^{137}Cs in the environment in Sweden [29].

Method

Activity concentration

The activity concentration of ^{210}Po, ^{238}U and ^{234}U in various food and foodstuffs were obtained from the research projects *Radiological implications of Swedish food consumption* and *NANOD - Natural Radioactivity in the Nordic Diet.* Washing and removal of the parts of the food that are not edible was performed of the samples. The activity concentration was measured using alpha spectrometry.

Activity concentration of ^{210}Po in diet containing animal protein and lacto-ovo vegetarian diet was collected from the research project *Radiological implications of Swedish food consumption*. Lunch and dinner samples for both diets were collected from a restaurant at Sahlgrenska University Hospital. The difference in committed effective dose estimated from the different diets was investigated.

Food consumption

The food consumption of the Swedish population was collected from the Swedish Board of Agriculture (Jordbruksverket), the Swedish National Food Agency (Livsmedelsverket) and the report *Svensk konsumtion av sjömat – en växande mångfald* from Research Institutes of Sweden [30]. Food consumption data for adults were found in the report *Food consumption and nutritive values, data up to 2016*, from the Swedish Board of Agriculture [31]. The data used are averages of the consumption during the years 2014, 2015 and 2016. In that report, the consumption data for fish were incomplete but were found in the report *Svensk konsumtion av sjömat – en växande mångfald* [30]. The food consumption data for children were extracted from *Food consumption and nutritive values, data up to 2016* [31] and *Svensk konsumtion av sjömat – en växande mångfald* [30] in combination with the Swedish National Food Agency reports *Livsmedels- och näringsintag bland barn i Sverige* [32] and *Livsmedelskonsumtion bland ungdomar i Sverige* [33]. The consumption data for children used in the calculation were fractions of the consumptions of adults. This was done because the consumption data for children were for food groups. For example, the proportion of the consumption of all vegetables could be applied to the consumption data for different vegetables available for adults.

A comparison of the committed effective dose for adults was done using different food consumption data. Consumption data were extracted from the United Nations Scientific Committee of the Effects of Atomic Radiation (UNSCEAR) 2008 report [3] and the Swedish National Food Agency report *Livsmedels- och näringsintag bland vuxna i Sverige* [34].

The difference in committed effective doses received by Swedish women and men due to different food consumption habits was investigated. The consumption data for women and men were collected from the report *Livsmedels- och näringsintag bland vuxna i Sverige* [34].

The food consumption data used in the calculations are presented in Appendix A: Food consumption data.

Dose estimation using dose coefficients

The committed effective doses from ^{210}Po, ^{238}U and ^{234}U were calculated using the dose coefficient for respective radionuclide extracted from ICRP 119 [19]. The committed effective dose E [Sv/y] was calculated as

$$E = \sum_i a_i \, c \, e_i, \tag{4}$$

where a_i is the activity concentration for radionuclide i [Bq/kg], c is the food consumption [kg/y] and e_i is the committed effective dose coefficient for radionuclide i [Sv/Bq].

Dose simulation by IMBA

Simulation of the dose from ^{210}Po was performed by varying the GI uptake fraction, the transfer rate between stomach and small intestine and the tissue weighting factors. The GI uptake fraction values used in the simulation are shown in Table 2 and are extracted from the study of biokinetics of polonium in man by Henricsson et al. [23].

Table 2: GI uptake fraction for polonium [23].

GI uptake fraction, f_1
0.46
0.51
0.56

Transfer rates in HATM were used to variate the transport between stomach and small intestine. The transfer rate for women and men were used to examine the sex dependence in dose. The transfer rates are shown in Table 3 and are collected from ICRP 100 [15].

Table 3: Transfer rate between stomach and small intestine [15].

Type of content in the GI tract	Transfer rate for women, $[d^{-1}]$	Transfer rate for men, $[d^{-1}]$
Solids	13.71	19.2
Caloric liquids	24	32
Non-caloric liquids	48	48
Total diet	15.16	20.54

Tissue weighting factors were found in ICRP 133 (2016) and were used in the simulation to compare with the weighting factors implemented in IMBA, originating from ICRP 68 (1994). The weighting factors from ICRP 68 are the ones used in the calculation of the present

committed effective dose coefficients for the public [19]. The weighting factors from ICRP 68 are shown in Table 4 [36] and factors from ICRP 133 are shown in Table 5 [35].

Table 4: Tissue weighting factors from ICRP 68 (1994) [36].

Tissue	w_T
Gonads	0.20
Red marrow, colon, lung, stomach	0.12
Bladder, breast, liver, oesophagus, thyroid, remainder*	0.05
Skin, bone surface	0.01

**Remainder: adrenals, brain, small intestine, kidney, muscle, pancreas, spleen, thymus, uterus.*

Table 5: Tissue weighting factors from ICRP 133 (2016) [35].

Tissue	w_T
Active bone marrow, breast, colon, lung, stomach, remainder tissues*	0.12
Gonads	0.08
Urinary bladder, oesophagus, liver, thyroid	0.04
Bone endosteum, brain, salivary glands, skin	0.01

**Remainder tissues includes adrenals, extrathoracic regions of the respiratory tract, gall bladder, heart, kidneys, lymphatic nodes, muscle, oral mucosa, pancreas, prostate, small intestine, spleen, thymus, uterus/cervix.*

Simulation of biokinetic models in SAAM II and Ecolego

To investigate the impact of the committed effective dose due to new developments in the biokinetic models, the distribution and retention of polonium in the human body was simulated by building HATM and the systemic model in SAAM II. To give a more accurate dose assessment for the Swedish population, the committed effective dose coefficient for ^{210}Po was calculated and used in the dose estimation.

The transfer coefficients needed were collected from ICRP 100 [15] for HATM and from ICRP 137 [18] for the systemic model for polonium. The simulated intake was 1 Bq ^{210}Po and was given in the compartment for oral cavity in HATM. To simulate both fast and slow motion of the swallowed activity, *oral cavity* was divided into two compartments. The transport of an ingested material is characterised by fast motion to 90% and by slow motion to 10% [15]. Therefore, 0.9 Bq ^{210}Po was given to the compartment for fast motion and 0.1 Bq ^{210}Po was given to the compartment for slow motion. The two compartments for the oral cavity are connected to one compartment for oesophagus each (fast and slow) and then they both connect to one compartment for the stomach. The two models were connected by letting the activity in *small intestine* in HATM flowing to *plasma 1* in the systemic model. Reabsorption from blood to the gastrointestinal tract was simulated by an activity flux between *liver 1* and *small intestine*.

The transfer rate $\lambda_{SI,B}$ from small intestine to blood was calculated as

$$\lambda_{SI,B} = \frac{f_{SI}\lambda_{SI,RC}}{1-f_{SI}}, \quad (5)$$

where $f_{SI} = 0.5$ is the absorbed fraction from small intestine to blood and $\lambda_{SI,RC}$ is the transfer rate between small intestine and right colon [15]. $\lambda_{SI,B}$ was calculated to 6 d^{-1}. To include the physical decay of ^{210}Po, every compartment was added an outflow equalling the decay constant of the radionuclide, i.e. $\lambda_{^{210}Po} = 0.0072$ d^{-1} [37]. The model and the transfer coefficients used are shown in Appendix B: The model used in SAAM II and Ecolego.

The software GraphPad Prism was used to fit the retention data to a sum of exponential curves. The retention curves were integrated, using the integration limit 50 years to get the time integrated activity. Using the methodology in ICRP 133 [35], the committed effective dose coefficient for ^{210}Po, applicable for the public, was calculated. The coefficient applicable for workers was calculated by using $f_{SI} = 0.1$ and was compared with the coefficient calculated by ICRP [18]. This comparison was done to verify the calculations.

^{210}Po decays to the stable nuclide ^{206}Pb through alpha particle emission. The energy of the alpha particle is 5.30 MeV and the yield is 1 [8]. The radiation weighted S coefficient $S_w(r_T \leftarrow r_S)$ was calculated for female and male, respectively, as

$$S_w(r_T \leftarrow r_S) = w_\alpha E_\alpha Y_\alpha \Phi(r_T \leftarrow r_S), \quad (6)$$

where r_T and r_S are the target and source region, respectively, $w_\alpha = 20$ is the radiation weighting factor for alpha particles, E_α is the energy of the alpha particle, Y_α is the yield of the decay and $\Phi(r_T \leftarrow r_S)$ is the specific absorbed fraction [35]. For the compartment *other* including several source regions r_S, $\Phi(r_T \leftarrow r_S)$ was calculated as

$$\Phi(r_T \leftarrow other) = \frac{1}{M_{other}} \sum_{r_S} M_{r_S} \Phi(r_T \leftarrow r_S), \quad (7)$$

where M_{other} is the total mass of the source regions included in the compartment *other* and M_{r_S} is the mass of source region r_S. The S coefficients are presented in Appendix C: S coefficients for **^{210}Po**. The committed equivalent dose coefficient $h(r_T)$ in target region r_T was calculated for female and male as

$$h^F(r_T) = \sum_{r_S} \tilde{a}(r_S)\, S_w^F(r_T \leftarrow r_S), \quad (8)$$

$$h^M(r_T) = \sum_{r_S} \tilde{a}(r_S)\, S_w^M(r_T \leftarrow r_S)\,, \tag{9}$$

where $\tilde{a}(r_S)$ is the integrated activity and $S_w^F(r_T \leftarrow r_S)$ and $S_w^M(r_T \leftarrow r_S)$ are the S coefficients for female and male, respectively. The target regions extrathoracic region, lung, colon and lymphatic nodes consist of several target tissues and for each target tissue, a fractional weighting factor is needed to be added to the equivalent dose coefficient. The committed effective dose coefficient e was calculated as

$$e = \sum_T w_T \left(\frac{h_T^F + h_T^M}{2}\right), \tag{10}$$

where w_T is the weighting factor for tissue T.

To verify the results from SAAM II, the software Ecolego was used to perform the biokinetic simulation.[3]

Interpolation maps

The software ArcGIS 10.6 was used to produce interpolation maps from discrete dose rate data. The method *Empirical Bayesian Kriging* (EBK) was used. A manual for the procedure of making the interpolation map was produced and tested using dose rate data over an area in Kvarntorp, Kumla municipality in Sweden, called Kvarntorpshögen. Interpolated dose rate maps were produced using 30% and 50% of the data, respectively. To examine the accuracy of the interpolation method, interpolated values were then compared with measured values in respective coordinate.

[3] The simulation in Ecolego was carried out by Mats Isaksson; professor at the Department of Radiation Physics, Institute of Clinical Sciences, Sahlgrenska Academy, Gothenburg University.

Results

Dose estimation using dose coefficients

The calculated committed effective doses from ^{210}Po, ^{238}U, ^{234}U and the sum of those three radionuclides are shown in Table 6-Table 8. The committed effective dose from ^{210}Po in different diets are shown in Table 9.

Table 6: Committed effective doses calculated using the dose coefficients from ICRP 119 [19] and food consumption data from the Swedish Board of Agriculture [31], the Swedish National Food Agency [32, 33] and the report Svensk konsumtion av sjömat – en växande mångfald [30]. The given uncertainties are calculated using 95% confidence interval. For adults the uncertainties include uncertainties in activity concentration and for children the uncertainties include uncertainties in activity concentration and food consumption.

Age group	Committed effective dose [µSv/y]			
	^{210}Po	^{238}U	^{234}U	Sum
Children 4-5 years	120 ± 10	0.33 ± 0.08	0.39 ± 0.08	120 ± 10
Children 10-12 years	86 ± 9	0.33 ± 0.09	0.37 ± 0.04	87 ± 9
Children 15 years	75 ± 7	0.34 ± 0.08	0.39 ± 0.08	76 ± 7
Children, average	94 ± 9	0.33 ± 0.08	0.38 ± 0.07	94 ± 9
Adults	76 ± 2	0.38 ± 0.04	0.45 ± 0.03	77 ± 2

Table 7: Committed effective doses for adults calculated using the dose coefficients from ICRP 119 [19] and different consumption data [3, 30, 31, 34]. The given uncertainties are calculated using 95% confidence interval. The uncertainties in the three comparing effective doses include uncertainties in activity concentration. The uncertainty of the effective dose calculated using consumption data from the Swedish National Food Agency also includes uncertainties in food consumption.

Origin of food consumption data	Committed effective dose [µSv/y]			
	^{210}Po	^{238}U	^{234}U	Sum
The Swedish Board of Agriculture and *Svensk konsumtion av sjömat – en växande mångfald*	76 ± 2	0.38 ± 0.04	0.45 ± 0.03	77 ± 2
The Swedish National Food Agency	150 ± 20	0.34 ± 0.09	0.50 ± 0.07	150 ± 20
UNSCEAR 2008	160 ± 7	0.41 ± 0.05	0.47 ± 0.03	160 ± 7

Table 8: Committed effective doses for Swedish women and men calculated using the dose coefficients from ICRP 119 [19] and the consumption data from the Swedish National Food Agency report Livsmedels- och näringsintag bland vuxna i Sverige [34]. The given uncertainties are calculated using 95% confidence interval. The given uncertainties include uncertainties in activity concentration and food consumption.

Sex	Committed effective dose [µSv/y]			
	^{210}Po	^{238}U	^{234}U	Sum
Female	140 ± 20	0.29 ± 0.08	0.40 ± 0.06	140 ± 20
Male	160 ± 20	0.41 ± 0.10	0.58 ± 0.09	170 ± 20

Table 9: Committed effective doses from ^{210}Po for diet containing animal protein and lacto-ovo vegetarian diet, calculated using the dose coefficients from ICRP 119 [19]. The ranges of committed effective dose from lunch and dinner and the sum of the meals are shown for the diets. The given uncertainties are calculated using 95% confidence interval. The given uncertainties include uncertainties in activity concentration.

Diet	Committed effective dose from ^{210}Po [µSv/y]	
	Range of lunch and dinner	Sum
Diet containing animal protein	$[18 \pm 0.8; 37 \pm 3]$	58 ± 3
Lacto-ovo vegetarian diet	$[6.3 \pm 0.4; 6.9 \pm 0.3]$	13 ± 1

Dose simulation by IMBA

The committed effective doses received from ^{210}Po simulated by IMBA using different GI uptake fractions are shown in Figure 4. The committed effective dose tends to increase linearly with the GI uptake fraction.

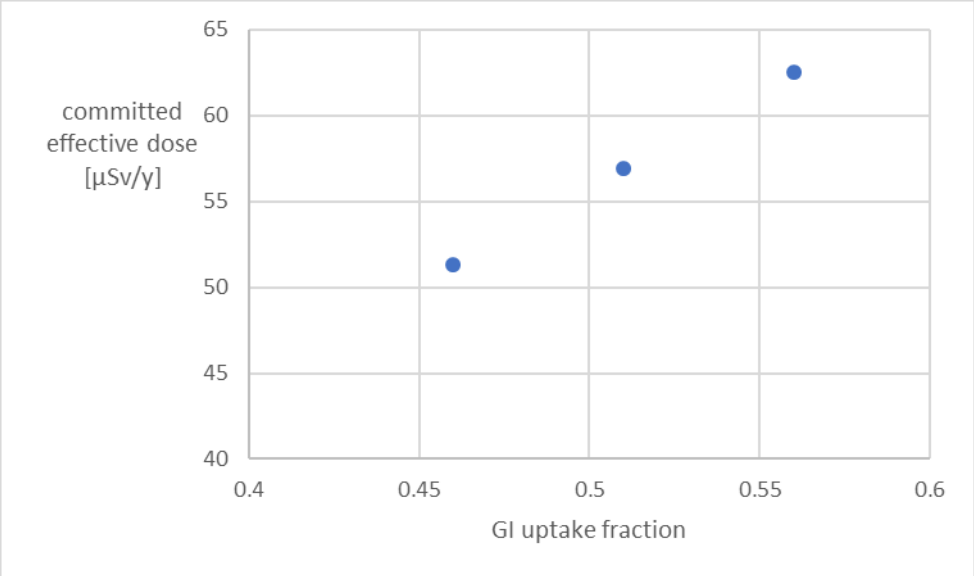

Figure 4: Committed effective dose received from ^{210}Po as a function of GI uptake fraction.

The simulated committed effective doses from ^{210}Po using different tissue weighting factors are shown in Table 10.

Table 10: The committed effective dose received from ^{210}Po using different tissue weighting factors.

Origin of tissue weighting factors	Committed effective dose [µSv/y]
ICRP 68 (1994)	56
ICRP 133 (2016)	69

By varying the transfer rate between stomach and small intestine, women are estimated to receive a slightly higher committed equivalent dose from ^{210}Po to stomach than men, see Table 11. When using the ICRP 68 weighting factors, the equivalent stomach dose in women was about 0.3% higher. This difference could be seen after minimum 2 years and for all types of food. When using the ICRP 133 weighting factors, the equivalent stomach dose in women was about 0.2% higher than in men and this difference could not be seen until after 16 years. Similar results were found for solid and caloric liquid food. For total diet, women were estimated to receive 0.3% higher equivalent dose to stomach after 15 years, using the ICRP 133 weighting factors.

Table 11: The difference in equivalent stomach dose to women compared with men, using different tissue weighting factors. The data correspond to the higher equivalent stomach dose in percentage received to women compared with men. The time after the exposure when the difference was noticeable are shown in brackets.

Tissue weighting factors	The difference in equivalent stomach dose estimated to women compared with men		
	Solid food	Caloric food	Total diet
ICRP 68 (1994)	0.3% (2 y)	0.3% (2 y)	0.3% (2 y)
ICRP 133 (2016)	0.2% (16 y)	0.2% (16 y)	0.3% (15 y)

Simulation of biokinetic models in SAAM II and Ecolego

The calculated committed effective dose coefficients for ^{210}Po are shown in Table 12.

Table 12: Committed effective dose coefficients from ^{210}Po (Sv/Bq) applicable for the public and for workers, calculated from simulations in SAAM II and Ecolego. For comparison, the committed effective dose coefficient for workers from ICRP 137 [18] and the coefficient for the public from ICRP 119 [19] are shown.

Origin of simulation data / Application	Committed effective dose coefficient			
	SAAM II	Ecolego	ICRP 137 (2017)	ICRP 119 (2012)
for the public	$1.42 \cdot 10^{-6}$	$1.27 \cdot 10^{-6}$	-	$1.20 \cdot 10^{-6}$
for workers	$1.91 \cdot 10^{-7}$	$1.93 \cdot 10^{-7}$	$1.80 \cdot 10^{-7}$	-

When comparing the results of the committed effective dose coefficient for workers from ICRP 137, the simulation data from SAAM II gave a 6% higher value and the data from Ecolego gave a 7% higher value. When comparing the results of the coefficient for the public from ICRP 119, the simulation data from SAAM II gave a 18% higher value and the data from Ecolego gave a 6% higher value.

The committed effective dose received to the Swedish adults, estimated using the calculated dose coefficients are shown in Table 13. The consumption data used in this calculation are extracted from the Swedish Board of Agriculture [31] and from *Svensk konsumtion av sjömaten - en växande mångfald* [30].

Table 13: Committed effective dose (μSv) to Swedish adults from NORM in food, estimated using the calculated dose coefficients from the simulations in SAAM II and Ecolego. The consumption data used are extracted from the Swedish Board of Agriculture [31] and from Svensk konsumtion av sjömaten - en växande mångfald [30]. The effective doses from ^{238}U and ^{234}U were calculated using the dose coefficients from ICRP 119 [19].

Origin of simulation data / Committed effective dose (μSv)	SAAM II	Ecolego
from ^{210}Po	90 ± 2	81 ± 2
total (considering ^{238}U and ^{234}U as well)	91 ± 2	81 ± 2

Interpolation maps

The interpolated dose rate map is shown in Figure 5. The produced manual for interpolation using the Empirical Bayesian Kriging method is shown in Appendix D: ArcGIS manual for interpolation using the Empirical Bayesian Kriging method.

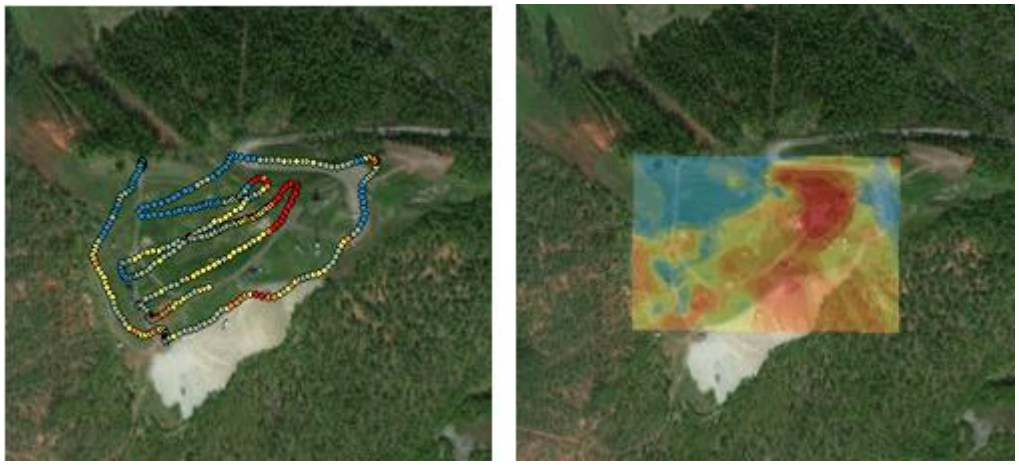

Figure 5: Discrete dose rate data are shown to the left and the interpolation map based on that data set is shown to the right.

The distribution of the discrete data used for the interpolation maps are shown in Figure 6. Predicted values from the interpolated maps based on 30% and 50% of the data are compared with measured values in Figure 7 and Figure 8. The predicted values from the interpolated map based on 30% of the data were in general highly overestimated. The most protruding predicted value is 2.4 times larger than the measured. Pearson coefficient was r = -0.0026 and $R^2 = 7 \cdot 10^{-6}$. From the map based on 50% of the data, the predicted values largely agreed with the measured values, with a few outliers. The most protruding value differs by 26% from the measured value. Pearson coefficient was r = 0.96 and $R^2 = 0.92$.

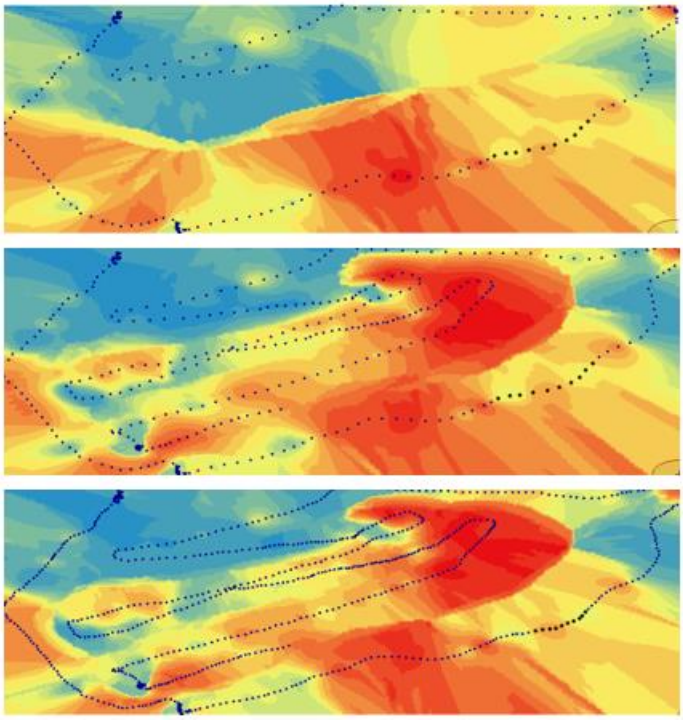

Figure 6: Distribution of the discrete dose rate data and appurtenant interpolation map. On top is shown 30% of the data, in the middle 50% of the data and at the bottom 100% of the data.

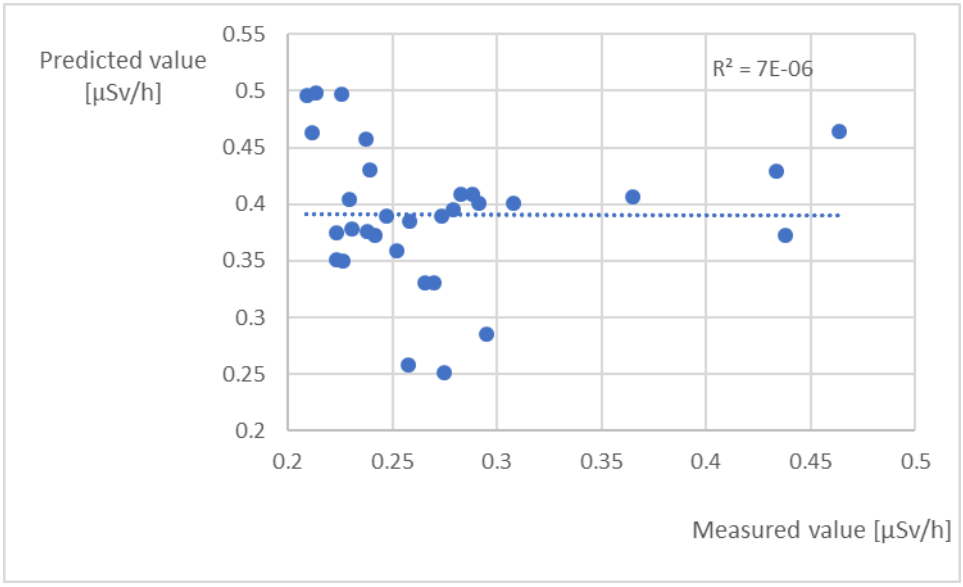

Figure 7: Predicted values from the interpolated dose rate map based on 30% of the data, plotted as a function of measured values.

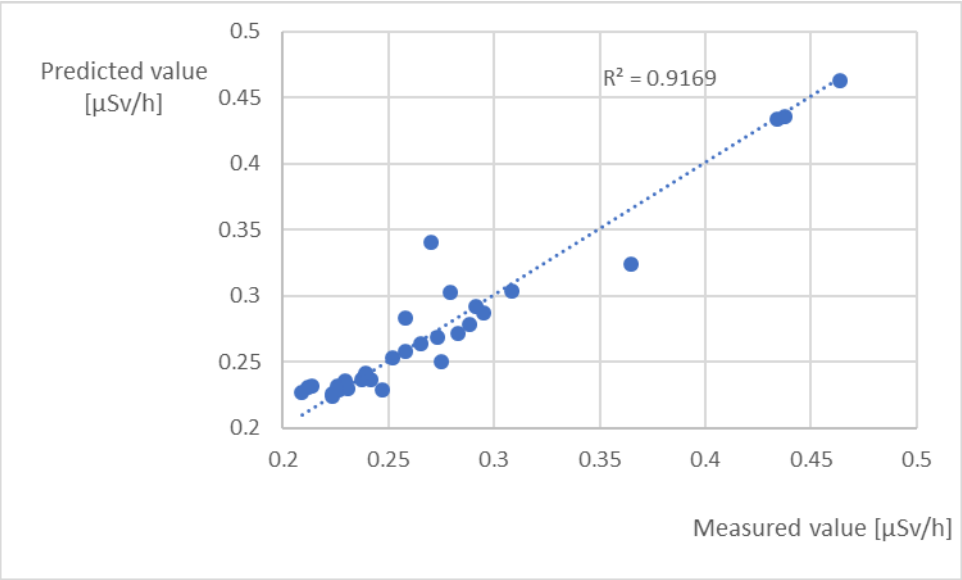

Figure 8: Predicted values from the interpolated dose rate map based on 50% of the data, plotted as a function of measured values.

Discussion

Dose estimation using dose coefficients

In this study, the received committed effective dose to the Swedish population from naturally occurring radionuclides in food and foodstuffs, was calculated. Using different food consumption data, the committed effective doses to adults were $[76 \pm 2; 160 \pm 7]$ μSv/y for ^{210}Po, $[0.34 \pm 0.05; 0.41 \pm 0.05]$ μSv/y for ^{238}U, $[0.45 \pm 0.03; 0.48 \pm 0.03]$ μSv/y for ^{234}U. The total committed effective dose to the Swedish adults was $[77 \pm 2; 160 \pm 7]$ μSv/y.

The data consisting of a combination of the consumption data from The Swedish Board of Agriculture and *Svensk konsumtion av sjömat – en växande mångfald*, were the most detailed data that were used. The data were produced by correcting the food production in Sweden with foreign trade and waste due to processing of raw materials. Information was given for consumption of different types of vegetable, fruit, meat, fish etc., while the other two consumption data sets that were used gave information on consumptions of food groups. One disadvantage with this data set is that the fish consumption data were presented as total consumption of the whole Swedish population. To get the consumption per capita, the data were divided by the population in Sweden in 2015. The population data were collected from the authority of statistics, SCB, and to consider that children eat less than adults and that the youngest children do not eat fish, the population under 15 years was not included. The data from the Swedish National Food Agency report Livsmedels- och näringsintag bland vuxna i Sverige have been collected by surveys where participants were filling in every food intake. This type of data collection results in the possibility of errors due to bad estimation of food consumption by the participant. Another disadvantage with this data set is that dishes are registered as the main ingredient of the dish, for example a meat pot is registered as meat. This means that other ingredients in the meat pot are not registered. In the UNSCEAR 2008 report, the mean food consumption for the world population is presented, giving the obvious disadvantage that these consumption data do not represent the Swedish population. The consumption data consisting of a combination of data from The Swedish Board of Agriculture and *Svensk konsumtion av sjömat – en växande mångfald*, were considered to be the most accurate. Therefore, the dose estimation out of this consumption data set was considered to be the best. One limitation of this data set is that no uncertainties are given, because this was considered to be too hard to estimate. This causes a misleading uncertainty in the dose, being too small when considering only the uncertainties in the measurement and sample preparation. The uncertainties in the doses were higher for children than those for adults, except for the doses calculated using data from the Swedish National Food Agency. This is because the consumption data from the Swedish National Food Agency were given with uncertainties which was propagated into the uncertainty in the dose.

The committed effective dose to the Swedish adults from NORM in food has been estimated by Statens strålskyddsinstitut (SSI) (the predecessor of the Swedish Radiation Safety Authority, SSM) to 200 μSv/y [4]. This estimation is based on global reference values for activity concentrations in food in combination with a world average food consumption. From

the results in the present study, the estimated committed effective dose to the Swedish adults was smaller, 77 ± 2 μSv/y, when using activity concentration representing Swedish food and consumption data representative for Swedes.

When comparing the committed effective doses to the world population, presented in UNSCEAR 2000 [7], with the committed effective doses to the Swedish population calculated in this study, the doses received from ^{210}Po to adults are very similar, 76 ± 2 μSv/y to the Swedish adults vs. 70 μSv/y to the world population. The average of the committed effective doses from ^{210}Po to Swedish children is 94 ± 9 μSv/y compared with the world average of 100 μSv/y. The committed effective doses received from ^{238}U and ^{234}U were larger for the Swedish population than for the world population, as can be seen in Table 1.

Comparing the doses calculated in the Norwegian study [5] to the doses estimated in this study it can be seen that the adult Norwegian people are receiving a committed effective dose from ^{210}Po of 120 μSv/y compared with 76 ± 2 μSv/y calculated in this study.

When comparing lacto-ovo vegetarian and animal protein containing diet, the dose difference is large. Swedish people who eat a diet including animal protein receive an almost 4.5 times greater committed effective dose from ^{210}Po than those who eat a lacto-ovo vegetarian diet. The reason for this is that the levels of ^{210}Po in general is much higher in meat and fish than in vegetable food. These results were based on meals collected from a restaurant. These food samples consisted of cooked food and foodstuff, in comparison with the other samples that were raw. The committed effective dose estimated from the cooked meals were much smaller than the doses estimated from raw samples. This could be a result of the cooking effect. The cooking effect is the impact in amount of a radionuclide due to heating of the food. It has been shown that the concentration of ^{210}Po in different foods, both can increase and decrease due to cooking [38]. A decrease can occur as a result of ^{210}Po evaporating due to its volatility and an increase can occur if there is loss of water which in turn leads to a higher concentration [38]. In the present study, it seems that the overall cooking effect decreased the amount of ^{210}Po. The amount of ^{210}Po is also affected by storage of the food before cooking. If using frozen food, the amount of the radionuclide can be lower compared with fresh food, due to physical decay (half-life of 138 d). Another factor contributing to the lower committed effective dose estimated from the cooked food, is that the food consumption per day was considered to consist of lunch and dinner, since there were the only such samples collected. The estimated committed effective doses should be somewhat higher if other meals during the day were included.

The difference between female and male showed that a 20% larger dose was received by Swedish men. The natural cause of this is that men eat more because of the larger energy need, but also because of differences in food habits. The consumption data show that Swedish men eat 60% more meat, 10% less vegetables and 40% less fruits than Swedish women. For fish, which gives the highest contribution of the committed effective dose, men have a 16% higher consumption than women.

Dose simulation by IMBA

The GI uptake fraction values for ^{210}Po extracted from the study of biokinetics of polonium in man by Henricsson et al. [23] result in estimated committed effective doses in the range [51.3; 62.5] μSv/y to Swedish adults. This gives a difference in committed effective dose of $\pm$ 9% compared with the corresponding value, using the GI uptake fraction defined by ICRP. In the study by Henricsson et al., the GI uptake fraction is estimated to 0.46 and the other two GI uptake fractions from the study, are collected from earlier studies (Thomas et al, 2001 and Hunt and Rumney, 2007). The GI uptake fraction is by ICRP considered to be 0.5 since 1993 when it was changed from 0.1 [23]. When taking the GI uptake fraction to be 0.5, the dose is 55.8 μSv/y, using IMBA. As the GI uptake fraction has been estimated to values both higher and lower than the one stated by ICRP, indicates that 0.5 may be a proper estimation. One difficulty in estimating the GI uptake fraction for polonium is the occurrence of ^{210}Po in the body due to intake of the nuclide every day via ingestion. This background level must be considered when studying the kinetics of ^{210}Po, which was the cases in the studies by Thomas et al and Hunt and Rumney [23]. In these two studies, volunteers were eating caribou and crab meat, respectively. Henricsson et al. examined the kinetics of ^{209}Po in the body by letting volunteers ingest a known amount of the nuclide. When using a nuclide that is not naturally present in the body, there was no background level disturbing the measured radioactivity.

The biological half-life was estimated in the studies by Henricsson et al. (31 $\pm$ 5.5 d), Leggett and Eckerman (38 $\pm$ 1 d), and Hunt and Rumney (42 $\pm$ 1 d) and they all got values lower than the half-life stated by ICRP (50 d) [23]. In IMBA, there is no possibility to change the biological half-life. Therefore, no estimation was done of the impact this could have on the committed effective dose to the Swedish population.

When using different tissue weighting factors in the simulation in IMBA, the results showed that the new weighting factors from ICRP 133 result in a higher estimate of the committed effective dose from ^{210}Po, 69 μSv/y, compared with 56 μSv/y when using the factors from ICRP 68. This is an increase of 23% and shows the importance of an update of the committed effective dose coefficient for ^{210}Po, using the tissue weighting factors from ICRP 133 instead of ICRP 68.

By varying the transfer rates between stomach and small intestine and studying the sex dependence in committed effective dose, very small differences were found, and women received a higher committed equivalent stomach dose than men.

Simulation of biokinetic models in SAAM II and Ecolego

The calculated committed effective dose coefficient for workers were 6-7% higher than that in ICRP 137 [18]. The greatest challenge in the calculation of the coefficient, using the simulations from SAAM II, was to get an accurate integration of the activity in the compartments. The curve fitting software GraphPad Prism was not able to find good fits for some of the compartments. For example, for women and $f_{SI} = 0.1$, GraphPad Prism was not

able to determine the parameters in the best fitted curve for the compartments *kidney 2*, *spleen*, *red marrow*, *plasma 3* and *gonads*. For most of the compartments, R^2 was 0.99 but for *skin* R^2 was 0.94, for *plasma 1* R^2 was 0.78 and for *bone surface* R^2 was 0.95. Similar problems were present for men and when using $f_{SI} = 0.5$. Ecolego, on the other hand, has a built-in function for integrating the activity in the compartments and therefore curve fitting is not included in the calculation [27].

Another advantage with Ecolego compared with SAAM II is the greater opportunities of solving the differential equations of the simulated model. Ecolego uses models that can solve stiff problems, i.e. models with largely variating transfer factors [27]. Since this is the case in this study, the results from Ecolego can be suggested to be more accurate than those from SAAM II. The different methods of solving the differential equations in SAAM II and Ecolego can be the reason for the difference in the calculated committed effective dose coefficients for the public. The coefficient calculated using the simulation data from SAAM II was 18% higher than the old coefficient from ICRP 119 [19] and when using the simulation data from Ecolego, the coefficient was 6% higher. When comparing the integrated activities for each compartment, there were large differences between the results from SAAM II and Ecolego. In 64% of the source organs (*blood, red marrow, kidney, liver, spleen, urinary bladder contents* and *other*) Ecolego gives a 13-18% higher integrated activity, compared with SAAM II. For the rest of the source organs, Ecolego gives lower values: 18-21% lower for *bone surface* and 27-33% lower for *skin* and *gonads*. This displays the difficulty of the integration.

The estimated committed effective dose received by the Swedish adults was 91 ± 2 μSv/y using the coefficient calculated from the data from SAAM II and 81 ± 2 μSv/y using the coefficient calculated from the data from Ecolego. The consumption data used in this estimation are extracted from the Swedish Board of Agriculture [31] and from *Svensk konsumtion av sjömaten - en växande mångfald* [30]. When using the old committed effective dose coefficient from ICRP 119 [19], the estimated dose is 77 ± 2 μSv/y. The results of this study suggest that the new development in the biokinetic models for polonium is leading to a 5-18% higher committed effective dose to Swedish adults from NORM in food.

Interpolation maps

The interpolated dose rate maps were obtained from ArcGIS 10.6. The interpolation was carried out using the Empirical Bayesian Kriging method, since the Kriging method has been used in an earlier study when interpolating the levels of ^{137}Cs in the environment in Sweden.

When comparing the measured values with the predicted received from the interpolation using 30% of the data, it could be seen that the estimation was largely overestimated for most of the values. That data set (see Figure 6) is distributed as a line in a form of an ellipse, compared with the 50% and 100% data sets which include values distributed within that ellipse. This is probably the reason for the bad agreement between the predicted and the measured values. Pearson coefficient was r = -0.0026 and $R^2 = 7 \cdot 10^{-6}$, indicates a low correlation. This shows the importance of having a data set that covers the area of which the interpolation is carried out

on. The predicted values from the interpolated dose rate map using 50% of the data was compared with the measured values. Because the distribution of the 50% and 100% data are the same, this comparison would act as a good indication of how well the Empirical Bayesian Kriging method works for interpolation of discrete dose rate data. High correlation was found, where Pearson coefficient was $r = 0.96$ and $R^2 = 0.92$. The predicted values extracted from the dose rate map produced from 50% of the data are largely in agreement with the measured values, suggesting this method works well.

Conclusion

The committed effective dose received by the Swedish population from NORM in food was estimated to 77 ± 2 μSv/y for adults and 94 ± 9 μSv/y for children. The Swedes eating an animal protein including diet receive 4.5 times higher committed effective dose compared with those eating a lacto-ovo vegetarian diet, because of the general higher content of ^{210}Po in fish and shellfish than in vegetable food. The overall effect of cooking led to a decrease in amount of ^{210}Po. Swedish men receive 20% higher committed effective dose compared with Swedish women, due to different food habits.

When varying the GI uptake fraction for ^{210}Po extracted from recent data, the estimate of the committed effective dose received by Swedish adults differed by $\pm$ 9% from the dose calculated using the GI uptake fraction defined by ICRP. The updated tissue weighting factors from ICRP 133 gave a 23% higher estimate of the committed effective dose from ^{210}Po compared with the old factors from ICRP 68, which are the ones used in the calculation of the dose coefficient in ICRP 119. When using the sex dependent transfer rates between stomach and small intestine collected from ICRP 100, women received a higher committed equivalent dose to the stomach compared with men.

In this study, the biokinetics of ^{210}Po was simulated and the results suggest that the new development in the biokinetic models lead to a 5-18% higher estimate of the committed effective dose from NORM in food received by Swedish adults.

Interpolation maps were done using the Empirical Bayesian Kriging method in the software ArcGIS 10.6. Measured and predicted values in respective coordinate were in good agreement, suggesting this method works well for this purpose.

Acknowledgements

I would like to thank my supervisors Dr. Francisco Piñero García and Prof. Mats Isaksson for their help and dedication throughout this work.

The study was supported by the Swedish Radiation Safety Authority (SSM) and the Nordic Nuclear Safety Research (NKS).

Reference list

1. IAEA. *Natural Radioactivity in Food: Experts Discuss Harmonizing International Standards*. 2017, last update date: 2018-05-14, access date: 2018-10-12; available from: https://www.iaea.org/newscenter/news/natural-radioactivity-in-food-experts-discuss-harmonizing-international-standards.
2. IAEA. *Radiation in Everyday Life*. 2017, last update date: 2017, access date: 2018-10-12; available from: https://www.iaea.org/Publications/Factsheets/English/radlife.
3. UNSCEAR, *Sources and Effects of Ionizing Radiation, UNSCEAR 2008 Report.* 2010.
4. Statens strålskyddsinstitut, *SSI Rapport 2007:02, Strålmiljön i Sverige.* 2007.
5. VKM, Alexander, J., Brantsæter A.L., Brunborg G., Fæste C.K., Jaworska A., et al., *Risk assessment of radioactivity in food. Opinion of the Scientific Steering Committee of the Norwegian Scientific Committee for Food Safety, VKM report 2017:25,* 2017.
6. Das, B., Deb, A., and Chowdhury, S., *Radiological Impact of some Common Foods of Southern of West Bengal, India.* Radiat Prot Dosimetry, p. 169-178. 2018.
7. UNSCEAR, *UNSCEAR 2000.* Health Phys, p. 314. 2000.
8. Chu, S.Y.F., Ekström, L.P., Firestone, R.B., *The Lund/LBNL Nuclear Data Search*. 1999. access date: 2018-12-03; available from: http://nucleardata.nuclear.lu.se/toi/nuclide.asp?iZA=840210.
9. Diaz-Frances, I., et al., *210Po in the diet at Seville (Spain) and its contribution to the dose by ingestion.* Radiat Prot Dosimetry, p. 271-6. 2016.
10. Persson, B.R. and Holm, E., *Polonium-210 and lead-210 in the terrestrial environment: a historical review.* J Environ Radioact, p. 420-9. 2011.
11. Atwood, D.A., *Radionuclides in the Environment*. John Wiley & Sons Ltd. 2010.
12. Isaksson, M., Rääf, C. L., *Environmental radioactivity and emergency preparedness*. Taylor & Francis Group, LLC. 2017.
13. Breustedt, B., Giussani, A., and Noßke, D., *Internal dose assessments – Concepts, models and uncertainties.* Radiation Measurements, p. 49-54. 2018.
14. ICRP, *Limits for Intakes of Radionuclides by Workers. ICRP Publication 30 (Part 2).* 1980.
15. ICRP, *Human Alimentary Tract Model for Radiological Protection. ICRP Publication 100.* 2006.
16. ICRP, *Occupational Intakes of Radionuclides: Part 1. ICRP Publication 130.* 2015.
17. ICRP, *Occupational Intakes of Radionuclides: Part 2. ICRP Publication 134.* 2016.
18. ICRP, *Occupational Intakes of Radionuclides: Part 3. ICRP Publication 137.* 2017.
19. ICRP, *Compendium of Dose Coefficients based on ICRP Publication 60. ICRP Publication 119.* 2012.
20. ICRP, *Age-dependent Doses to Members of the Public from Intake of Radionuclides - Part 2 Ingestion Dose Coefficients. ICRP Publication 67.* 1993.
21. Leggett, R.W. and Eckerman, K.F., *A systemic biokinetic model for polonium.* Sci Total Environ, p. 109-25. 2001.
22. Li, W.B., et al., *Internal dose assessment of 210Po using biokinetic modeling and urinary excretion measurement.* Radiat Environ Biophys, p. 101-10. 2008.
23. Henricsson, C.F., et al., *A biokinetic study of 209Po in man.* Science of the Total Environment, p. 384-389. 2012.
24. Leggett, R.W., *Reliability of the ICRP's dose coefficients for members of the public. 1. Sources of uncertainty in the biokinetic models.* Radiat Prot Dosimetry, p. 199-213. 2001.
25. James, C.A., et al., *IMBA Professional Plus, User Manual, Appendix A: Technical Basis.* 2005.
26. Barrett, P.H., et al., *SAAM II: Simulation, Analysis, and Modeling Software for tracer and pharmacokinetic studies.* Metabolism, p. 484-92.1998.

27. Ecolego Website*, Ecolego Features*. 2019, access date: 2019-01-05; available from: http://ecolego.facilia.se/ecolego/show/Ecolego.
28. ArcGIS, *ArcGIS Help Library, ArcGIS 10.6*. 2017.
29. Almgren, S., et al., *GIS supported calculations of (137)Cs deposition in Sweden based on precipitation data.* Sci Total Environ, p. 804-13. 2006.
30. Ziegler, F., Bergman, K., *Svensk konsumtion av sjömaten - en växande mångfald, RISE Research Institutes of Sweden.* 2017.
31. Jordbruksverket, *Livsmedelskonsumtion och näringsinnehåll, Uppgifter till och med 2016.* 2017.
32. Livsmedelsverket, *Riksmaten – barn 2003, Livsmedels- och näringsintag bland barn i Sverige.* 2006.
33. Livsmedelsverket, *Riksmaten ungdom 2016-17, Livsmedelskonsumtion bland ungdomar i Sverige*. 2018.
34. Livsmedelsverket, *Riksmaten vuxna 2010-11, Livsmedels- och näringsintag bland vuxna i Sverige.* 2012.
35. ICRP, *The ICRP computational framework for internal dose assessment for reference adults: specific absorbed fractions. ICRP Publication 133.* 2016.
36. ICRP, *Dose Coefficients for Intakes of Radionuclides by Workers. ICRP Publication 68.* 1994.
37. ICRP, *Nuclear Decay Data for Dosimetric Calculations. ICRP Publication 107.* 2008.
38. Díaz-Francés, I., Díaz-Ruiz, J., Manjón, G., García-Tenorio, R., *210Po Activity Concentrations in Cooked Marine Food.* Journal of Fisheries Sciences, 2017.
39. SCB. *Statistikdatabasen, Befolkning efter ålder och kön. År 1860-2017,* access date: 2018-12-12; available from: http://www.statistikdatabasen.scb.se/pxweb/sv/ssd/START__BE__BE0101__BE0101A/BefolkningR1860/?rxid=15c4f7cb-6833-4707-b02e-4d8176fc7f2e.

Appendix A: Food consumption data

In Appendix A the food consumption data, used in the dose estimation, are presented.

Table A1: Food consumption data for Swedish adults from the Swedish Board of Agriculture [31]. The listed consumption data are averages of the consumptions during the years 2014, 2015 and 2016.

Food/foodstuff	*kg/y*
Plum	3.13
Apple	10.99
Cucumber	6.27
Potatoes	54.33
Zucchini	8.80
Carrots	10.83
Broccoli	4.67
Cauliflower	1.53
Flour	8.17
Blue Berries	4.83
Onions	9.03
Beetroot	1.93
Tomato	9.87
Milk	78.17
Egg	11.33
Mushroom	8.80
Chicken	20.87
Beef Mince	12.83
Yoghurt	31.4
Cabbage	4.67
Bananas	21.47
Pear	2.41
Bread	52.43
Oatmeal	3.53
Strawberries	4.83
Deer	1.67
Wild Boar	1.67
Sausage	14.73
Lamb	1.33
Orange	17.80
Pork	15.07
Turkey	20.87

Table A2: Food consumption data for Swedish adults from the report Svensk konsumtion av sjömaten - en växande mångfald [30]. To get the consumption per capita, the total fish consumption in Sweden year 2015 was divided by 8133874 (the Swedish population in 2015, including adults and children from 15 years and up) [39].

Type of fish	*Consumption (kg/y)*
Herrings	1.77
Blue Mussel	0.05
Cod	2.13
Hake	0.11
Saithe	0.68
Mackerel	0.77
Shrimp	0.77
Pike-perch	0.0007
Plaice	0.20

Table A3: Relative food consumption data for children of ages 4, 12 and 15 years received from the Swedish National Food Agency [32, 33] compared with consumption data for adults received from the Swedish Board of Agriculture [31] and the report Svensk konsumtion av sjömaten - en växande mångfald [30]. The consumption data for children are averages between girls and boys. The uncertainties are given as SEM.

Food	*Relative food consumption compared with adults*		
	4 y	*12 y*	*15 y*
vegetables	0.30±0.01	0.80±0.02	0.95±0.02
Root vegetables	0.23±0.02	0.51±0.04	0.46±0.03
fruits and berries	0.59±0.02	0.36±0.02	0.42±0.02
potatoes	0.53±0.01	0.56±0.02	0.60±0.02
rice & grains	0.98±0.07	1.39±0.17	1.96±0.23
bread	0.31±0.01	0.43±0.01	0.47±0.01
milk	1.13±0.07	1.36±0.09	1.40±0.10
yoghurt	1.06±0.09	0.76±0.04	0.66±0.04
meat	0.66±0.02	0.59±0.02	0.62±0.02
birds	0.21±0.02	0.52±0.04	0.59±0.04
sausage	0.57±0.02	1.07±0.04	1.03±0.04
fish & shellfish	0.56±0.04	0.68±0.06	0.90±0.07
egg	0.19±0.02	0.15±0.04	0.21±0.05

.

Table A4: Food consumption for women and men received from the Swedish National Food Agency [34]. The uncertainties are given as SEM.

Food	*Women (kg/y)*	*Men (kg/y)*	*Average (kg/y)*
vegetables & mushrooms	53.66±0.97	49.64±1.07	52.20±0.72
fruits & berries	53.66±1.28	38.33±1.57	46.72±1.01
potatoes	26.65±0.81	48.55±1.57	36.14±0.87
root vegetables	8.40±0.40	7.30±0.53	8.03±0.32
bread	27.38±0.48	37.23±0.72	31.76±0.43
milk	50.74±1.98	64.97±3.23	56.94±1.80
egg	5.11±0.32	5.11±0.44	5.11±0.26
fish	13.51±0.46	15.70±0.70	14.24±0.40
birds	7.30±0.37	8.40±0.56	8.03±0.33
meat	18.25±0.40	29.2±0.70	23.00±0.41
yoghurt	31.76±2.06	32.85±3.19	32.12±1.83
oat meal	12.41±1.28	15.33±2.02	14.24±1.14
sausage	5.48±0.32	10.22±0.53	7.67±0.30

Table A5: World average food consumption received from the UNSCEAR 2008 report [3].

Food	*Consumption (kg/y)*
milk	105
meat	50
grains	140
vegetables	60
fruit & root vegetables	170
fish	15

Appendix B: The model used in SAAM II and Ecolego

In Appendix B, the model is shown (Figure B1) and the transfer coefficients used in the simulation in SAAM II are presented (Table B1).

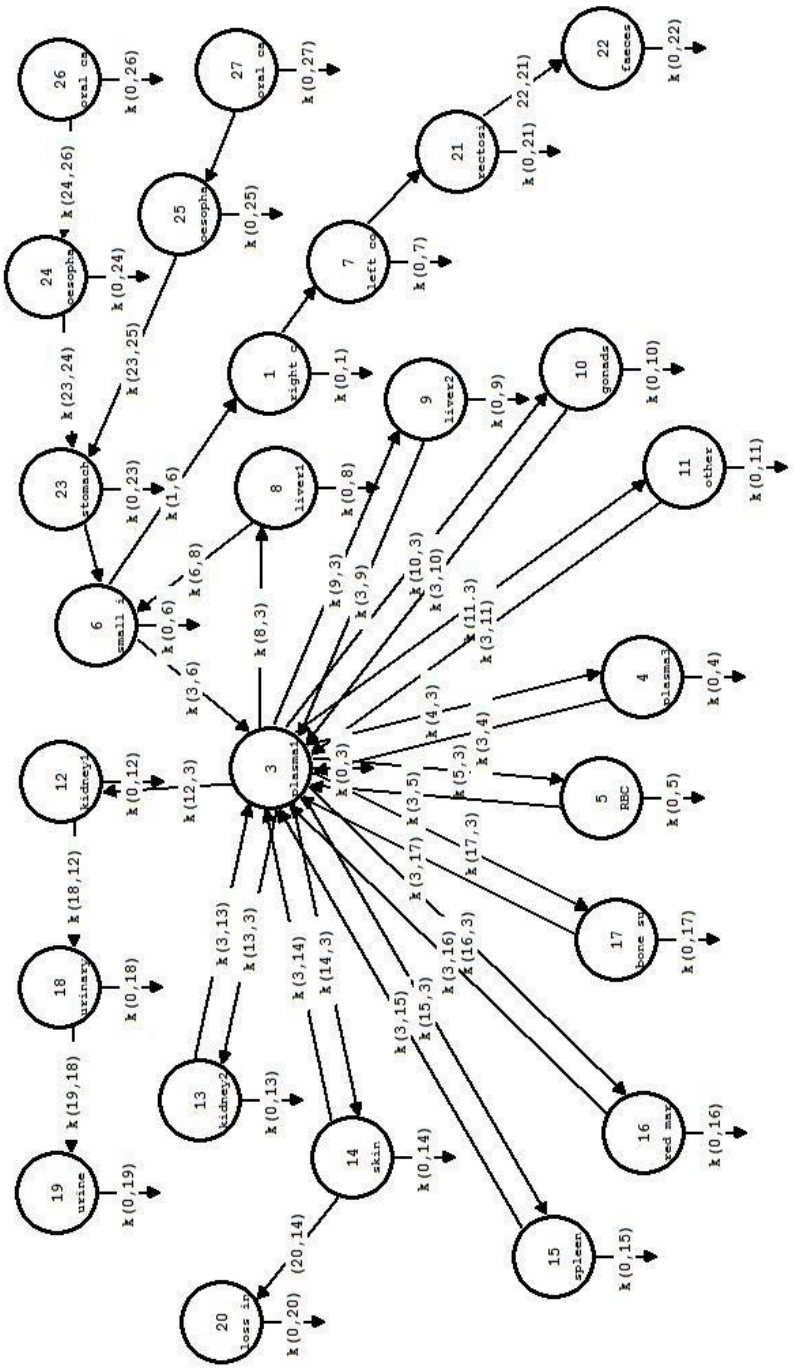

Figure B1: The systemic model for polonium connected to HATM used as model in SAAM II and Ecolego.

Table B1: The transfer coefficients [d^{-1}] used in the simulation in SAAM II. The coefficients in HATM are collected from ICRP 100 [15] and the coefficients in the systemic model are collected from ICRP 137 [18]. The coefficients for women are listed before those for men, when the values are different.

k(0,1)	physical decay ← right colon	0.0072
k(0,10)	physical decay ← gonads	0.0072
k(0,11)	physical decay ← other	0.0072
k(0,12)	physical decay ← kidney 1	0.0072
k(0,13)	physical decay ← kidney 2	0.0072
k(0,14)	physical decay ← skin	0.0072
k(0,15)	physical decay ← spleen	0.0072
k(0,16)	physical decay ← red marrow	0.0072
k(0,17)	physical decay ← bone surface	0.0072
k(0,18)	physical decay ← urinary bladder	0.0072
k(0,19)	physical decay ← urine	0.0072
k(0,20)	physical decay ← hair, sweat	0.0072
k(0,21)	physical decay ← rectosigmoidal	0.0072
k(0,22)	physical decay ← faeces	0.0072
k(0,23)	physical decay ← stomach	0.0072
k(0,24)	physical decay ← oesophagus slow	0.0072
k(0,25)	physical decay ← oesophagus fast	0.0072
k(0,26)	physical decay ← oral cavity slow	0.0072
k(0,27)	physical decay ← oral cavity fast	0.0072
k(0,3)	physical decay ← plasma 1	0.0072

k(0,4)	physical decay ← plasma 3	0.0072	
k(0,5)	physical decay ← RBC	0.0072	
k(0,6)	physical decay ← small intestine	0.0072	
k(0,7)	physical decay ← left colon	0.0072	
k(0,8)	physical decay ← liver 1	0.0072	
k(0,9)	physical decay ← liver 2	0.0072	
k(1,6)	right colon ← small intestine	6	
k(10,3)	gonads ← plasma 1	0.05	0.1
k(11,3)	other ← plasma 1	32.35	
k(12,3)	kidney 1 ← plasma 1	5	
k(13,3)	kidney 2 ← plasma 1	5	
k(14,3)	skin ← plasma 1	5	
k(15,3)	spleen ← plasma 1	2	
k(16,3)	red marrow ← plasma 1	4	
k(17,3)	bone surface ← plasma 1	1.5	
k(18,12)	urinary bladder ← kidney 1	0.173	
k(19,18)	urine ← urinary bladder	12	
k(20,14)	sweat, hair ← skin	0.0069	
k(21,7)	rectosigmoidal ← left colon	1.5	2
k(22,21)	faeces ← rectosigmoidal	1.5	2

Table B1 continuing

k(23,24)	stomach ← oesophagus slow	2160	
k(23,25)	stomach ← oesophagus fast	12343	
k(24,26)	oesophagus slow ← oral cavity slow	7200	
k(25,27)	oesophagus fast ← oral cavity fast	7200	
k(3,10)	plasma 1 ← gonads	0.0139	
k(3,11)	plasma 1 ← other	0.099	
k(3,13)	plasma 1 ← kidney 2	0.099	
k(3,14)	plasma 1 ← skin	0.0069	
k(3,15)	plasma 1 ← spleen	0.099	
k(3,16)	plasma 1 ← red marrow	0.099	
k(3,17)	plasma 1 ← bone surface	0.0231	
k(3,4)	plasma 1 ← plasma 3	0.099	
k(3,5)	plasma 1 ← RBC	0.099	
k(3,6)	plasma 1 ← small intestine	0.6667	
k(3,9)	plasma 1 ← liver 2	0.099	
k(4,3)	plasma 3 ← plasma 1	4	
k(5,3)	RBC ← plasma 1	6	
k(6,23)	small intestine ← stomach	15.16	20.57
k(6,8)	small intestine ← liver 1	0.139	
k(7,1)	left colon ← right colon	1.5	2
k(8,3)	liver 1 ← plasma 1	17.5	
k(9,3)	liver 2 ← plasma 1	17.5	

Appendix C: S coefficients for ^{210}Po

In Appendix C, the S coefficients for ^{210}Po are presented. Acronyms for source and target regions are listed in *Table C1*.

Table C1: Acronyms for source and target regions [35].

Source/target region	*Acronym*
Stomach	St stem
Small intestine	SI stem
Right colon	RC stem
Left colon	LC stem
Rectosigmoid colon	RS stem
ET1 basal cells	ET1 bas
ET2 basal cells	ET2 bas
Extrathoracic lymph nodes	LN ET
Bronchi basal cells	bronch bas
Bronchi secretary cells	bronch sec
Bronchiolar secretary cells	bchiol sec
Alveolar-interstitial	AI
Thoracic lymph nodes	LN th
Red marrow	R-marrow
Endosteal cells	Endost-BS
Pituitary gland	p-gland
Salivary glands	s-glands
Heart wall	Ht-wall
Gall bladder	GB-wall
Urinary bladder	UB-wall
Systemic lymph nodes	LN-sys
Cortical bone surface	C-bone-S
Trabecular bone surface	T-bone-S

Table C2: Female S coefficients $(Sv\ (Bq\ s)^{-1})$ for ^{210}Po.

Source / Target	blood	C-bone-S	T-bone-S	R-marrow	kidneys
oral mucosa	1.24E-13	0	0	0	0
oeosophagus	7.87E-13	0	0	0	0
St stem	7.87E-13	0	0	0	0
SI stem	8.55E-13	0	0	0	0

RC stem	8.31E-13	0	0	0	0
LC stem	8.31E-13	0	0	0	0
RS stem	8.31E-13	0	0	0	0
ET1 bas	1.24E-13	0	0	0	0
ET2 bas	1.24E-13	0	0	0	0
LN ET	2.25E-13	0	0	0	0
bronch bas	6.77E-13	0	0	0	0
bronch sec	6.77E-13	0	0	0	0
bchiol sec	6.77E-13	0	0	0	0
AI	2.33E-12	0	0	0	0
LN th	2.25E-13	0	0	0	0
R-marrow	6.39E-13	0	2.59E-12	1.0E-11	0
Endost-BS	2.42E-13	2.92E-12	1.96E-11	4.5E-12	0
brain	1.51E-13	0	0	0	0
eye lence	0	0	0	0	0
p-gland	1.24E-13	0	0	0	0
tongue	1.24E-13	0	0	0	0
tonsills	1.24E-13	0	0	0	0
s-glands	1.24E-13	0	0	0	0
thyroid	5.24E-13	0	0	0	0
breast	1.24E-13	0	0	0	0
thymus	1.24E-13	0	0	0	0
Ht-wall	5.84E-13	0	0	0	0
adrenals	6.60E-13	0	0	0	0
liver	9.39E-13	0	0	0	0
pancreas	7.05E-13	0	0	0	0
kidneys	9.52E-13	0	0	0	4.76E-11

spleen	1.27E-12	0	0	0	0
GB-wall	1.24E-13	0	0	0	0
ureters	1.24E-13	0	0	0	0
UB-wall	8.33E-14	0	0	0	0
ovaries	5.38E-13	0	0	0	0
testes	0	0	0	0	0
prostate	0	0	0	0	0
uterus	1.24E-13	0	0	0	0
LN-sys	2.25E-13	0	0	0	0
skin	2.10E-13	0	0	0	0
adipose	6.64E-14	0	0	0	0
muscle	9.95E-14	0	0	0	0

Table C3: Female S coefficients $(Sv\ (Bq\ s)^{-1})$ for ^{210}Po, continuing.

Source / Target	liver	ovaries	skin	spleen	UB cont	other
oral mucosa	0	0	0	0	0	3.53E-13
oeosophagus	0	0	0	0	0	2.85E-13
St stem	0	0	0	0	0	6.29E-13
SI stem	0	0	0	0	0	6.29E-13
RC stem	0	0	0	0	0	5.47E-13
LC stem	0	0	0	0	0	5.39E-13
RS stem	0	0	0	0	0	5.33E-13
ET1 bas	0	0	0	0	0	3.15E-13
ET2 bas	0	0	0	0	0	6.28E-13
LN ET	0	0	0	0	0	3.33E-13
bronch bas	0	0	0	0	0	6.94E-13

bronch sec	0	0	0	0	0	7.83E-13
bchiol sec	0	0	0	0	0	5.85E-13
AI	0	0	0	0	0	5.07E-13
LN th	0	0	0	0	0	3.33E-13
R-marrow	0	0	0	0	0	3.08E-13
Endost-BS	0	0	0	0	0	4.6E-13
brain	0	0	0	0	0	3.39E-13
eye lence	0	0	0	0	0	3.52E-13
p-gland	0	0	0	0	0	3.42E-13
tongue	0	0	0	0	0	3.42E-13
tonsills	0	0	0	0	0	3.42E-13
s-glands	0	0	0	0	0	3.42E-13
thyroid	0	0	0	0	0	3.08E-13
breast	0	0	0	0	0	3.42E-13
thymus	0	0	0	0	0	3.42E-13
Ht-wall	0	0	0	0	0	3.03E-13
adrenals	0	0	0	0	0	2.96E-13
liver	9.39E-12	0	0	0	0	0
pancreas	0	0	0	0	0	2.92E-13
kidneys	0	0	0	0	0	0
spleen	0	0	0	9.07E-11	0	0
GB-wall	0	0	0	0	0	3.43E-13
ureters	0	0	0	0	0	3.42E-13
UB-wall	0	0	0	0	2.01E-13	3.45E-13
ovaries	0	1.44E-09	0	0	0	0
testes	0	0	0	0	0	0
prostate	0	0	0	0	0	0

uterus	0	0	0	0	0	3.42E-13
LN-sys	0	0	0	0	0	3.34E-13
skin	0	0	7.01E-12	0	0	0
adipose	0	0	0	0	0	3.47E-13
muscle	0	0	0	0	0	3.44E-13

Table C4: Male S coefficients $(Sv\ (Bq\ s)^{-1})$ *for* ^{210}Po.

Source / Target	blood	C-bone-S	T-bone-S	R-marrow	kidneys
oral mucosa	1.36E-13	0	0	0	0
oeosophagus	6.91E-13	0	0	0	0
St stem	6.91E-13	0	0	0	0
SI stem	7.49E-13	0	0	0	0
RC stem	7.58E-13	0	0	0	0
LC stem	7.58E-13	0	0	0	0
RS stem	7.58E-13	0	0	0	0
ET1 bas	1.36E-13	0	0	0	0
ET2 bas	1.36E-13	0	0	0	0
LN ET	1.79E-13	0	0	0	0
bronch bas	5.55E-13	0	0	0	0
bronch sec	5.55E-13	0	0	0	0
bchiol sec	5.55E-13	0	0	0	0
AI	1.80E-12	0	0	0	0
LN th	1.79E-13	0	0	0	0
R-marrow	4.88E-13	0	1.98E-12	7.6E-12	0
Endost-BS	1.86E-13	2.19E-12	1.46E-11	3.4E-12	0
brain	1.34E-13	0	0	0	0

eye lence	0	0	0	0	0
p-gland	1.36E-13	0	0	0	0
tongue	1.36E-13	0	0	0	0
tonsills	1.36E-13	0	0	0	0
s-glands	1.36E-13	0	0	0	0
thyroid	4.37E-13	0	0	0	0
breast	1.36E-13	0	0	0	0
thymus	1.36E-13	0	0	0	0
Ht-wall	4.40E-13	0	0	0	0
adrenals	5.88E-13	0	0	0	0
liver	7.20E-13	0	0	0	0
pancreas	5.88E-13	0	0	0	0
kidneys	8.05E-13	0	0	0	4.03E-11
spleen	1.04E-12	0	0	0	0
GB-wall	1.36E-13	0	0	0	0
ureters	1.36E-13	0	0	0	0
UB-wall	6.65E-14	0	0	0	0
ovaries	0	0	0	0	0
testes	1.83E-13	0	0	0	0
prostate	1.36E-13	0	0	0	0
uterus	0	0	0	0	0
LN-sys	1.79E-13	0	0	0	0
skin	1.47E-13	0	0	0	0
adipose	4.85E-14	0	0	0	0
muscle	7.99E-14	0	0	0	0

Table C5: Male S coefficients $(Sv\ (Bq\ s)^{-1})$ for ^{210}Po, continuing.

Source / Target	liver	skin	spleen	UB cont	testes	other
oral mucosa	0	0	0	0	0	2.95E-13
oeosophagus	0	0	0	0	0	2.28E-13
St stem	0	0	0	0	0	5.16E-13
SI stem	0	0	0	0	0	5.17E-13
RC stem	0	0	0	0	0	4.4E-13
LC stem	0	0	0	0	0	4.43E-13
RS stem	0	0	0	0	0	4.35E-13
ET1 bas	0	0	0	0	0	2.63E-13
ET2 bas	0	0	0	0	0	5.25E-13
LN ET	0	0	0	0	0	2.77E-13
bronch bas	0	0	0	0	0	5.83E-13
bronch sec	0	0	0	0	0	6.58E-13
bchiol sec	0	0	0	0	0	4.93E-13
AI	0	0	0	0	0	4.23E-13
LN th	0	0	0	0	0	2.77E-13
R-marrow	0	0	0	0	0	2.89E-13
Endost-BS	0	0	0	0	0	4.06E-13
brain	0	0	0	0	0	2.82E-13
eye lence	0	0	0	0	0	2.95E-13
p-gland	0	0	0	0	0	2.82E-13
tongue	0	0	0	0	0	2.82E-13
tonsills	0	0	0	0	0	2.82E-13
s-glands	0	0	0	0	0	2.82E-13
thyroid	0	0	0	0	0	2.53E-13
breast	0	0	0	0	0	2.82E-13

thymus	0	0	0	0	0	2.82E-13
Ht-wall	0	0	0	0	0	2.52E-13
adrenals	0	0	0	0	0	2.38E-13
liver	7.20E-12	0	0	0	0	0
pancreas	0	0	0	0	0	2.38E-13
kidneys	0	0	0	0	0	0
spleen	0	0	7.44E-11	0	0	0
GB-wall	0	0	0	0	0	2.83E-13
ureters	0	0	0	0	0	2.82E-13
UB-wall	0	0	0	1.60E-13	0	2.89E-13
ovaries	0	0	0	0	0	0
testes	0	0	0	0	4.56E-10	0
prostate	0	0	0	0	0	2.82E-13
uterus	0	0	0	0	0	0
LN-sys	0	0	0	0	0	2.77E-13
skin	0	4.90E-12	0	0	0	0
adipose	0	0	0	0	0	2.9E-13
muscle	0	0	0	0	0	2.87E-13

Appendix D: ArcGIS manual for interpolation using the Empirical Bayesian Kriging method

ArcGIS ArcMap 10.6 manual for interpolation using the Empirical Bayesian Kriging method

Preparation of the data file

Create a file in .csv format consisting of three columns: the longitude coordinates, the latitude coordinates and the data you want to interpolate i.e. dose rate or activity concentration.

How to import data into ArcMap

1. Click *Catalog* > *Folder connections* and right click to connect the catalog to the folder in your computer where your data are stored.

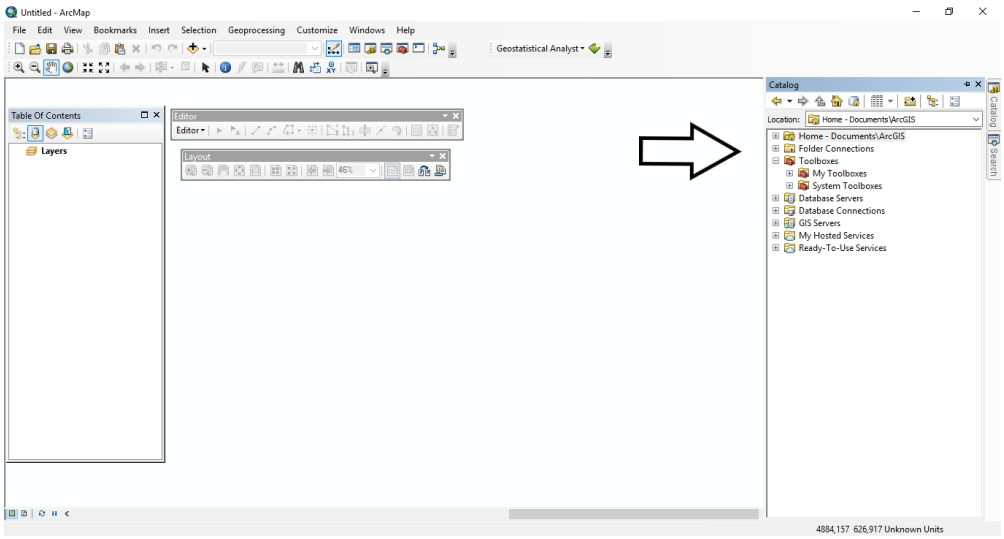

2. Click *Add data* and add the data file.

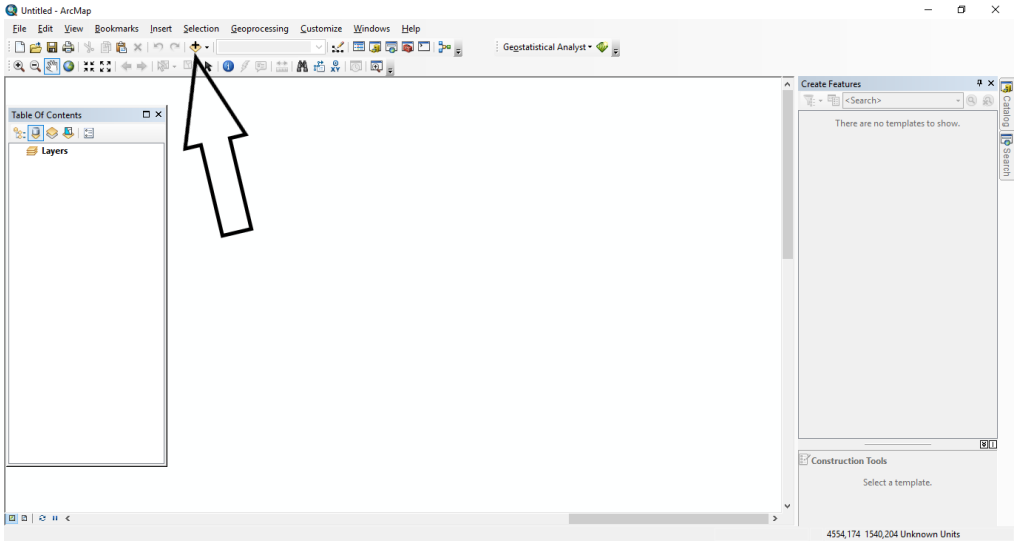

3. The added data file is now displayed in *Table of contents*. Right click on the data and choose *display XY data*. Make sure the longitude data are interpreted as X Field, the latitude data as Y Field and the dose rate/activity concentration data as Z Field. Click *Edit* > *Geographic coordinate systems* and choose the coordinate system your data are expressed in (WGS 84 is found in the folder *World*). After you have clicked *OK* twice, the data can now be shown graphically. It may pop up a box that says "your data has no object ID" – click *OK*.

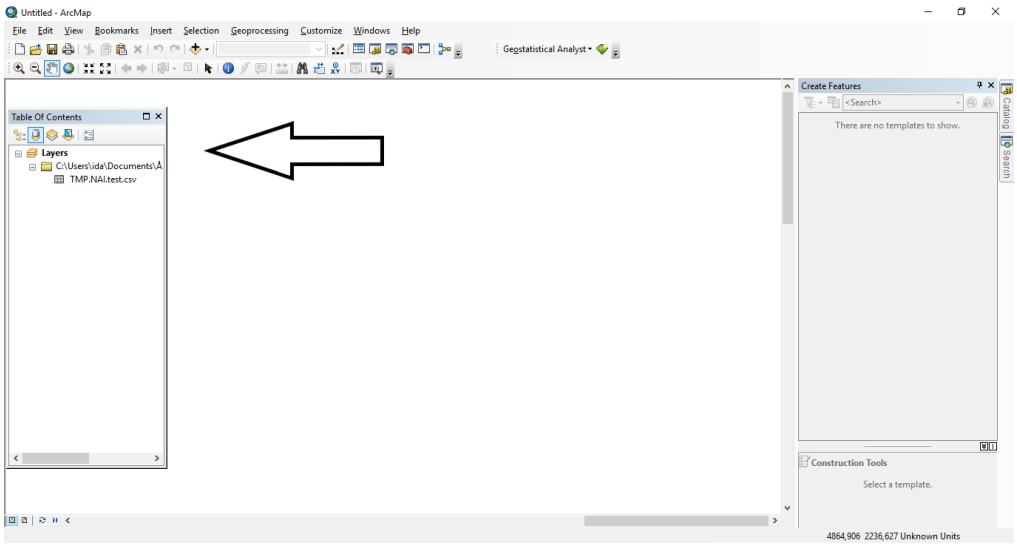

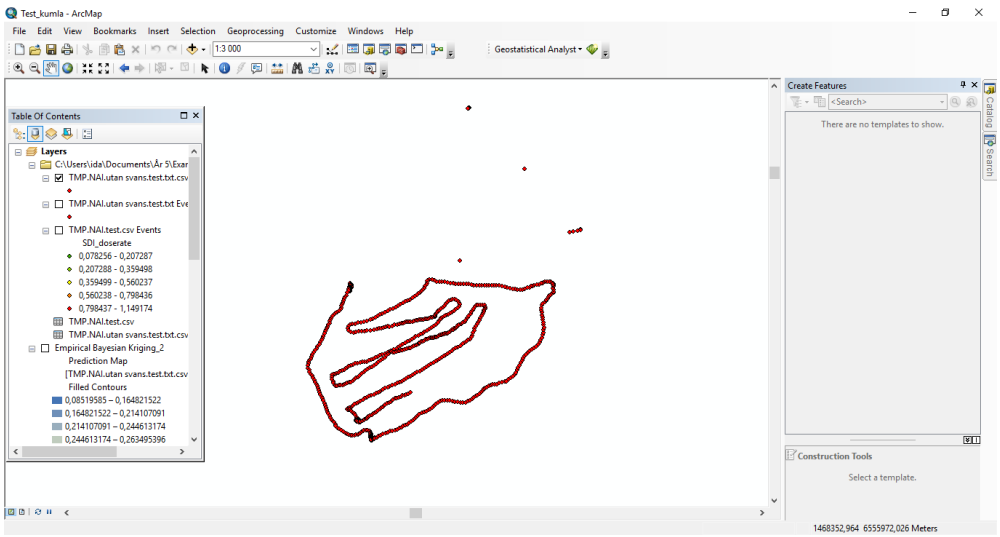

4. Import a geographical map by clicking *File* > *Add data* > *Add Basemap* and choose the map you prefer. The geographical map is now listed in *Table of contents* and must be at the bottom of the list, otherwise your dose rate data will not be shown in the graphical view.

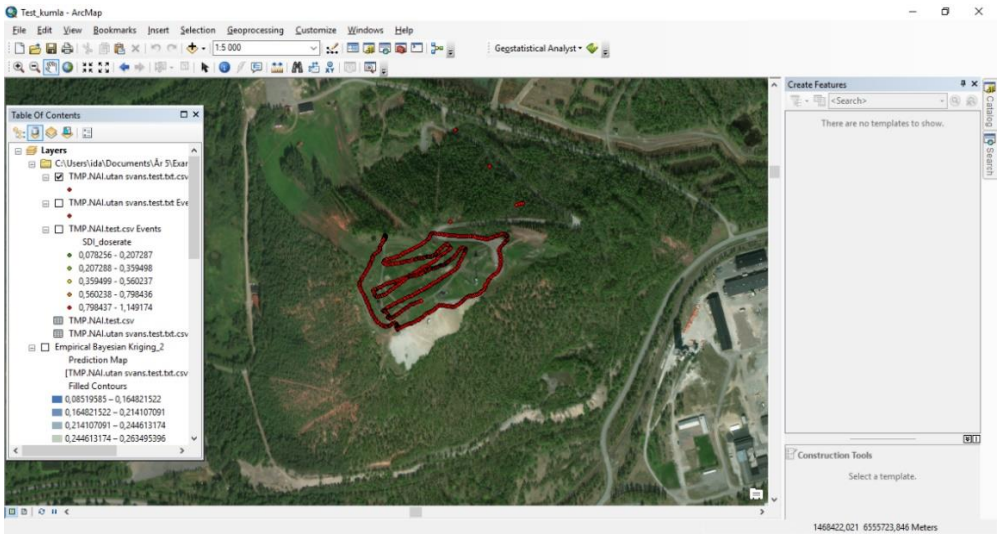

Interpolation using the Empirical Bayesian Kriging method

Using the *EBK* method, there are some options to make. In *EBK*, the data are divided into subsets to make the calculation faster [28]. The number of subsets can be selected by the user as well as the overlap factor and the number of simulations. The overlap factor is deciding to what extent the subsets are to be overlapping and the higher value the smoother the interpolation gets and the longer time it takes. The number of simulations, i.e. the number of simulated semivariogram per subsets, can be selected and the more simulations the more accurate gets the interpolation but the longer time it takes. In some geostatistical methods for interpolation, the data must be normal distributed. In *EBK*, there is an option for making the

data normal distributed by using a transformation (Empirical or Log Empirical). Anyway, there is no need to have normal distributed data when making a predicted surface map and therefore the choice should be to not make a transformation. There are three different types of functions, for fitting of the semivariogram, to choose between; Power, Linear and Thin Plate Spline. Power is default because it is relatively fast and give generally good accuracy. Linear can be chosen if the interpolation is to be faster and a bit less accurate and Thin Plate Spline is appropriate if there is a strong trend in the data.

The user can choose between standard circular or smooth circular when deciding which surrounding data points to be used for the prediction [28]. When using standard circular, the surrounding data points are chosen if they are within a certain radius (which can be chosen by the user). The largest and the smallest number of data points used in the calculation can be set by the user. When using smooth circular, one small ellipse and one larger outer ellipse are created. If the data points are inside the small ellipse, they are included for the prediction. The data points that are between the ellipses will be weighted with a factor between 0 and 1 before they are included in the calculation. Standard circular is the default method and smooth circular takes longer time.

Click *Customize* > *Extensions* and check the box for *Geostatistical Analyst*. Then click *Customize* > *Toolbars* > *Geostatistical Analyst* and the toolbar will appear on the workspace.

1. Click *Geostatistical Analyst* > *Geostatistical Wizard* and choose *Empirical Bayesian Kriging*.

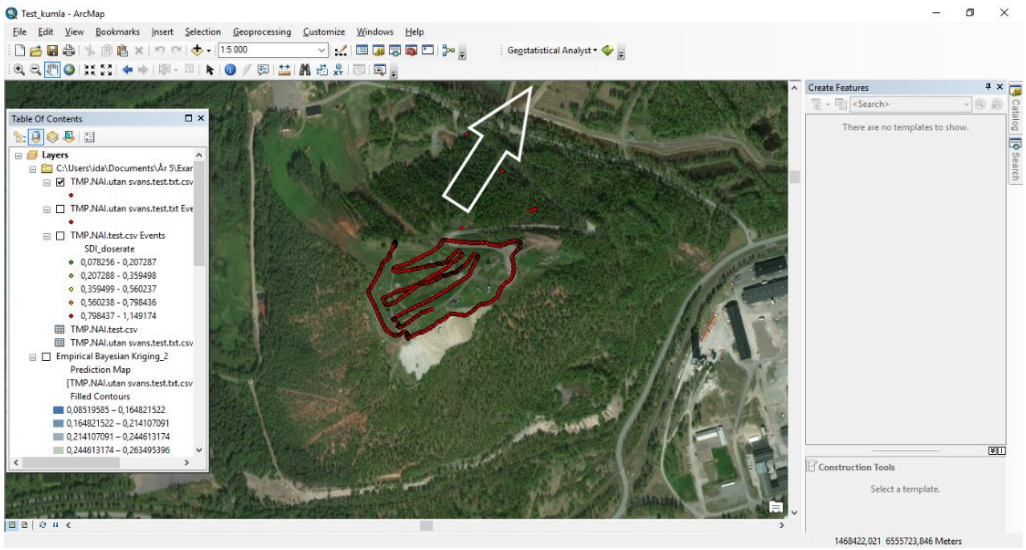

2. Select your data file followed by “Events” as your *Source Dataset* and the column with your dose rate/ activity concentration data as your *Data field*. Click *Next*.
3. A box will come up if your file consists of data points having the same coordinates, here you can choose to make the software taking the mean value of those points.
4. The next step is showing the *Method properties*, here you can change the properties or use the default selections. Click *Next*.
5. The last step is showing some statistics of the interpolation, click *Finish*.

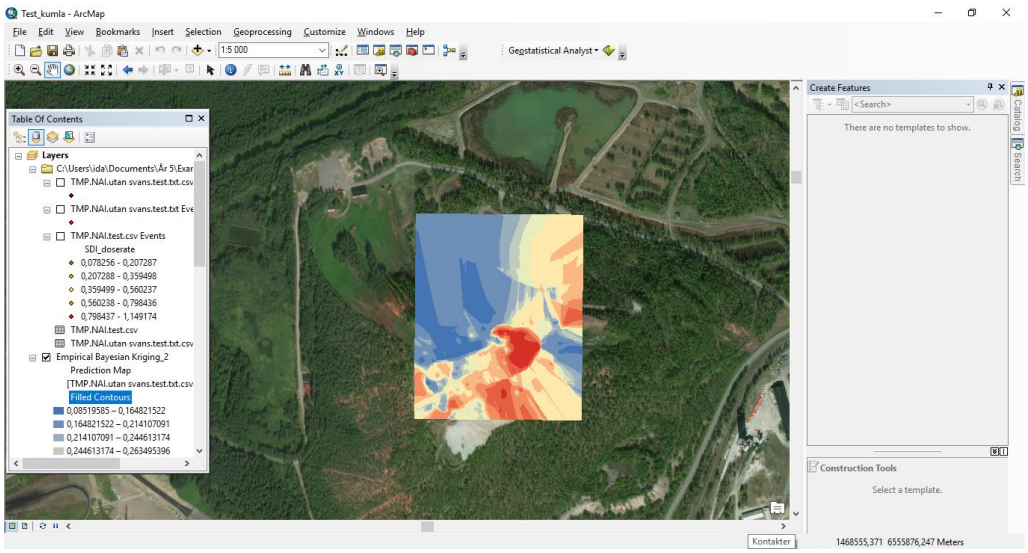

6. Unmark the box for your discrete data in the *Table of Contents*.
7. Double click on *Filled colours* under the *Empirical Bayesian Kriging Prediction Map* in the *Table of Contents*. Under the tab *Display* you can change the transparency of the predicted map.
8. Choose *Layout View* and Click *File* > *Export Map* to save your map as a file, for example in .png format.

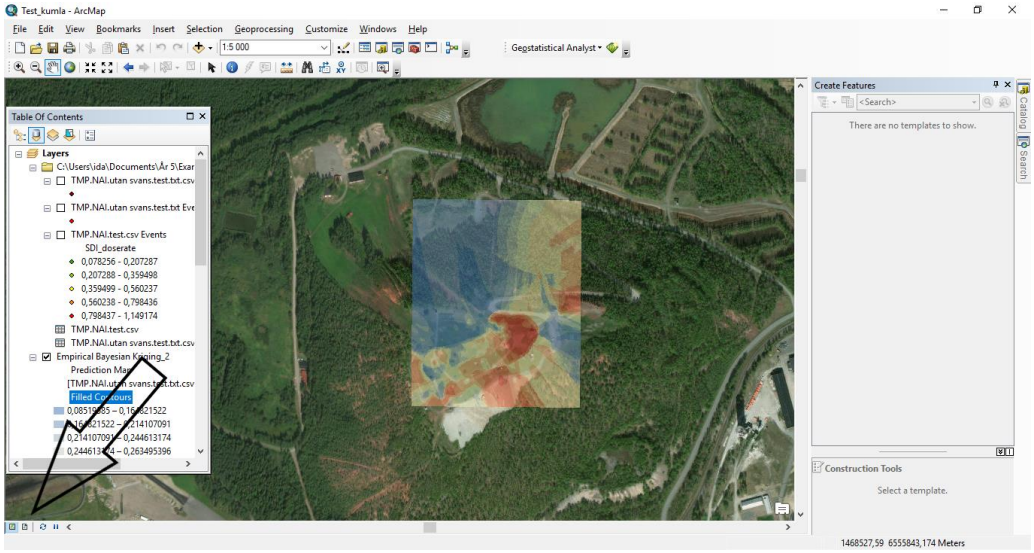

The finished interpolated map is shown below.